E2-2002-36

G. N. Afanasiev*, V. M. Shilov

CHERENKOV RADIATION VERSUS BREMSSTRAHLUNG IN THE TAMM PROBLEM

Submitted to «Journal of Physics D»

*E-mail: afanasev@thsun1.jinr.ru

1 Introduction

In 1934-1937, the Russian physicist P.A. Cherenkov performed a series of experiments under the suggestion of his teacher S.I. Vavilov. In them, photons emitted by Ra atoms passed through water. They induced the blue light observed visually. Applying an external magnetic field, Cherenkov recognized that this blue light was produced by secondary electrons knocked out by photons.

These experiments were explained by Tamm and Frank in 1937-1939 who attributed the above blue light to the radiation of a charge uniformly moving in medium with a velocity greater than the light velocity in medium.

Theoretically, when considering the Cherenkov radiation, one usually treats either the unbounded charge motion with a constant velocity (this corresponds to the so-called Tamm-Frank problem [1]) or the charge motion on a finite interval with an instantaneous acceleration and deceleration of a charge at the beginning and termination of its motion. This corresponds to the so-called Tamm problem [2]. The physical justification for the Tamm problem is as follows. A charge, initially uniformly moving in vacuum (where it does not radiate), penetrates into the transparent dielectric slab (where it radiates if the condition $\cos\theta_{Ch} = 1/\beta n$ for the Cherenkov angle is satisfied) and, finally, after leaving the dielectric slab, moves again in vacuum without radiating (we disregard the transition radiation at the boundaries of the dielectric slab). The appearance of radiation at the moment when a charge enters the slab and its termination at the moment when it leaves the slab are usually interpreted in terms of the instantaneous charge acceleration at one side of the slab and its instantaneous deceleration at its other side. Since the Tamm problem is more physical than the Tamm-Frank one, it is frequently used for the analysis of experimental data. Another possible application of the Tamm problem is the electron creation in some space point (nuclear β decay) with its subsequent absorption in another space point (nuclear β capture). Tamm obtained a remarkably simple analytic formula describing the intensity of radiation and interpreted it as the Cherenkov radiation on a finite interval [2].

Another viewpont on the nature of radiation observed by Cherenkov is due to S.I. Vavilov [3]. According to him, "We think that the most probable reason for the γ luminiscence is the radiation arising from the deceleration of Compton electrons. The hardness and intensity of γ rays in the experiments of P.A. Cherenkov were very large. Therefore, the number of Compton scattering events and the number of scattered electrons should be very considerable in fluids. The free electrons in a dense fluid should be decelerated at negligible distances. This should be followed by the radiation of the continuos spectrum. Thus, the weak visible radiation may arise, although the boundary of bremsstrahlung and its maximum should be located somewhere in the Roentgen region. It follows from this that the energy distribution in the visible region should rise towards the violet part of spectrum, and the blue-violet part of spectrum should be especially intensive" (our translation from Russian).

This Vavilov explanation of the Cherenkov effect has given rise to a number of

attempts (see, e.g., [4,5]) in which the radiation described by the Tamm formula was attributed to the interference of bremsstrahlungs (BS) arising at the start and end of motion.

On the other hand, the exact solution of the Tamm problem in a non-dispersive medium was found and analyzed in [6]. It was shown there that the Cherenkov shock wave exists side by side with BS waves and not in any case can be reduced to them. Then, how this fact can be reconciled with the results of [4,5] which describe experimental data quite satisfactorily? The possible explanation of this controversy is that the exact solution obtained in [6] was written out in the space-time representation, while the authors of [4, 5] operated with the Tamm formula related to the frequency representation. It might be happened that the main contribution to the exact solution of [6] describing the Cherenkov wave is due to the integration over the frequency region lying outside the visible part of the intensity spectrum. Then, in principle, the radiation in the visible part of spectrum could be described by the Tamm formula frequently used for the interpretation of experimental data.

The aim of this consideration is to resolve this controversy. We shall operate simultaneously in the spectral representation as authors of [4,5] did and in the time representation used in [6]. Instead of the original Tamm problem in which a charge exhibits instantaneous acceleration and deceleration, we consider a charge motion with a finite acceleration and deceleration and the uniform motion on the remaining part of a trajectory. This allows us to separate contributions from the uniform and non-uniform parts of a charge trajectory. Formerly, analytic and numerical results for the motion with the velocity change small as compared with the charge velocity itself were obtained in [7,8]. Unfortunately, the method used there does not work in the treated case, since the charge is accelerated from the state of rest up to acquiring the velocity close to that of light. Numerically, the smoothed Tamm problem with a large velocity change was considered in [9], but their authors did not aim to resolve there the above controversy between Refs. [4,5] and [6].

The plan of our exposition is as follows. In section 2, exact mathematical formulae describing the EMF and radiation intensity of a charge arbitrary moving in medium are presented. Various approximations needed for the subsequent exposition are discussed. Section 3 is devoted to the consideration of particular cases. At first (section (3.1)), the radiation arising from the pure decelerated (accelerated) charge motion in medium with arbitrary acceleration is considered. The corresponding analytic formulae and numerical results are presented. This particular case is realized in heavy-water nuclear reactors where the electrons arising from a β-decay, move with deceleration up to their complete stopping. In subsections 3.2 and 3.3, the analytic formulae are obtained desribing the radiation intensity from a charge whose trajectory includes accelerated, decelerated, and uniform parts. It is shown that contributions of accelerated and decelerated parts of a trajectory decrease when their lengths tend to zero (despite the fact that the acceleration is infinite in this limit). This means that the radiation intrensity described by the Tamm formula cannot be attributed to the interference of BS shock waves arising at the beginning and ter-

mination of a charge motion. In section 4, using the asymptotic behaviour of the Fresnel integrals, we rewrite formulae of section 3 in terms of elementary functions. This may be useful for the qualitative interpretations of calculations made in section 3. In section 5, we reconsider the original Tamm problem. It turns out that in the framework of the approximate solution found by Tamm, it is impossible to discriminate between the standard interpretation [2] of the Tamm intensity formula (which attributes observed radiation to the radiation of the uniformly moving charge with the velocity greater than light velocity in medium) and the one used in [4,5] (which associates observed radiation with the interference of BS shock waves). However, this discrimination is possible if we treat the Tamm problem using the exact time reprentation found in [6] and the spectral representation given in section 3.2. In fact, we prove that in some time interval, there exist the BS shock wave originating from the beginning of motion and the Cherenkov shock wave, and there is no BS shock wave originating from the termination of motion. Due to the lack of the second BS wave, there is no interference between these BS waves, and, as a consequence, the Cherenkov shock wave is not due to their interference. Further, the continuous transition from the smoothed Tamm problem studied in section 3.2 to the original Tamm problem shows that the latter does not include the contributions of instantaneous acceleration and deceleration. Thus, the above-mentioned alternative interpretation of the Cherenkov radiation is not sufficient. The discussion of the results obtained and their short resume are given in sections 6 and 7.

2 Main mathematical formulae

Let a point charge move along the z axis with a trajectory $z = \xi(t)$ in a non-dispersive medium with the refractive index n. Then, its charge and current densities are equal to

$$\rho = e\delta(x)\delta(y)\delta(z-\xi(t)), \quad j_z = ev(t)\delta(x)\delta(y)\delta(z-\xi(t)), \quad v = \frac{d\xi}{dt}.$$

We need also Fourier transforms of these densities

$$\rho(\omega) = \frac{e}{2\pi}\int \exp(-i\omega t)\rho(t)dt = \frac{e}{2\pi}\delta(x)\delta(y)\int \exp(-i\omega t)\delta(z-\xi(t))dt =$$

$$= \frac{e}{2\pi v}\delta(x)\delta(y)\exp(-i\omega\tau(z)), \quad j_z(\omega) = \frac{e}{2\pi})\delta(x)\delta(y)\exp(-i\omega\tau(z)), \qquad (2.1)$$

where $\tau(z)$ is the root of the equation $z - \xi(t) = 0$. It was assumed here that $v > 0$, that is, a charge moves in the positive direction of the z axis.
The Fourier transform of the vector potential corresponding to these densities at the space point x, y, z is equal to

$$A_z(\omega) = \frac{e}{2\pi c}\int \frac{dz'}{R}\exp(-i\psi), \qquad (2.2)$$

where $\psi = \omega\tau(z') + knR$ and $R = \sqrt{x^2 + y^2 + (z - z')^2}$ and $k = \omega/c$. The nonvanishing Fourier component of the magnetic field strength is

$$H_\phi(\omega) = \frac{iek_n r \sin\theta}{2\pi c} \int \frac{dz'}{R^2} \exp(-i\psi)(1 - \frac{i}{k_n R}). \tag{2.3}$$

Here $k_n = \omega/c_n$ and $c_n = c/n$ is the light velocity in medium. Outside the motion axis, the electric field strengths are obtained from the Maxwell equation

$$curl\vec{H}(\omega) = \frac{i\omega\epsilon}{c}\vec{E}(\omega). \tag{2.4}$$

This gives:

$$E_\theta(\omega) = -\frac{e\sin\theta}{\pi cn} \int \frac{dz'}{R^2} \exp(-i\psi)(1 - \frac{i}{k_n R}) +$$

$$\frac{iekr\sin\theta}{2\pi c} \int \frac{dz'(r - z'\cos\theta)}{R^3}(1 - \frac{3i}{k_n R} - \frac{3}{k_n R^2}) \exp(-i\psi). \tag{2.5}$$

The energy flux in the radial direction per unit time and per unit area of the observation sphere of the radius r is

$$S_r = \frac{d^2W}{r^2 d\Omega dt} = \frac{c}{4\pi} E_\theta(t) H_\phi(t).$$

The enery radiated for the whole charge motion is

$$\int_{-\infty}^{\infty} S_r dt = \frac{c}{4\pi} \int_{-\infty}^{\infty} dt E_\theta(t) H_\phi(t) = \frac{c}{2} \int_0^{\infty} d\omega [E_\theta(\omega) H_\phi^*(\omega) + E_\theta^*(\omega) H_\phi^*(\omega)]. \tag{2.6}$$

Usually, radial energy fluxes are related not to the unit area, but to the unit solid angle. For this, one should multiply Eq. (2.6) by r^2 (r is the radius of the observation sphere). Then,

$$r^2 \int_{-\infty}^{\infty} S_r dt = \int_0^{\infty} \sigma_r(\omega) d\omega,$$

where

$$\sigma_r(\theta) = \frac{d^2W}{d\Omega d\omega} = \frac{c}{2} r^2 [E_\theta(\omega) H_\phi^*(\omega) + E_\theta^*(\omega) H_\phi(\omega)]. \tag{2.7}$$

Substituting (2.3) and (2.5) into (2.7), one gets for the nonvanishing components of the energy fluxes

$$\sigma_r(\omega) = \frac{e^2 k^2 n r^4 \sin^2\theta}{4\pi^2 c} \times$$

$$\{\int \frac{dz'}{R^2}(\cos\psi_1 - \frac{\sin\psi_1}{k_n R}) \cdot \int \frac{r - z'\cos\theta}{R^3}[\cos\psi_1(1 - \frac{3}{k_n^2 R^2}) - \frac{3}{k_n R}\sin\psi_1] dz' +$$

$$+\int \frac{dz'}{R^2}(\sin\psi_1 + \frac{\cos\psi_1}{k_n R}) \cdot \int \frac{r - z'\cos\theta}{R^3}[\sin\psi_1(1 - \frac{3}{k_n^2 R^2}) + \frac{3}{k_n R}\cos\psi_1]dz'\}, \quad (2.8)$$

where $\psi_1 = \omega\tau(z') + kn(R-r)$. Equation (2.8) is very convenient, since it contains ψ_1 rather than ψ. For the observation distance r much larger than the motion interval $L = 2z_0$, the second term in ψ_1 is of the order $k_n z_0$ which is much smaller than $\psi \sim k_n r$. This fact greatly simplifies calculations for large frequencies. Equations (2.8) are exact and valid for arbitrary motion.

Since in real situations always $k_n r >> 1$ (for example, for $\lambda = 5 \cdot 10^{-5} cm, r = 100cm$ and $n = 1.5$, $k_n r$ is about 10^7), one can drop terms with $k_n R$ in denominators. Then,

$$\sigma_r(\omega) = \frac{e^2 k^2 n r^4 \sin^2\theta}{4\pi^2 c}[\int \frac{dz'\cos\psi_1}{R^2} \cdot \int \frac{(r - z')dz'\cos\theta}{R^3}\cos\psi_1 +$$

$$+\int \frac{dz'\sin\psi_1}{R^2} \cdot \int \frac{(r - z'\cos\theta)dz'}{R^3}\sin\psi_1]. \quad (2.9)$$

If, in addition, the motion interval L is much smaller than the radius r of the observaton sphere, one can disregard the ratios z'/r outside the ψ_1 function:

$$\sigma_r(\theta) = \frac{e^2 k^2 n \sin^2\theta}{4\pi^2 c}[(\int dz'\cos\psi_1)^2 + (\int dz'\sin\psi_1)^2]. \quad (2.10)$$

Let the motion interval L be finite. In the ψ_1 function, we develop R up to the second order w.r.t. z'/r:

$$\psi_1 = \omega\tau(z') - knz'\cos\theta + \frac{knz'^2\sin^2\theta}{2r}. \quad (2.11)$$

Since ψ_1 enters into sines and cosines, the last term in this expression can be neglected if $knz'^2\sin^2\theta/2r << 1$. Or, taking for $\sin\theta$ and z' their maximal values ($\sin\theta = 1, \quad z' = L$), one gets

$$\frac{knL^2}{2r} << 1. \quad (2.12)$$

In realistic conditions, this equation is not satisfied. For example, for

$$\lambda = 4 \cdot 10^{-5} cm, \quad L = 1cm, \quad r = 100cm \quad \text{and} \quad n = 1.5,$$

inequality (2.12) takes the form $10^3 << 1$. Complications arising from this fact were studied in [8,10]. However, here we are mainly interested in investigating effects arising from the charge acceleration and deceleration. Thus, in all concrete calculations, we deliberately disregard the last term in the expansion (2.11) of ψ_1. In this case, ψ_1 is reduced to

$$\psi_1 = \omega\tau(z') - knz'\cos\theta. \quad (2.13)$$

For the rectilinear motion, this approximation gives the famous Tamm formula

$$\sigma_T(\theta) = \frac{e^2}{\pi^2 cn}[\sin\theta \frac{\sin\omega t_0(1-\beta_n\cos\theta)}{\cos\theta - 1/\beta_n}]^2, \quad t_0 = \frac{z_0}{v} \quad \beta_n = \frac{v}{c_n}. \tag{2.14}$$

A question arises, why it is needed to use the approximate expression (2.13) although the numerical integration is rather easy [9]. One of the reasons is the same as for the use of the Tamm formula which does not work at realistic distances [8,10]. Despite this fact and due to its remarkable simplicity, the Tamm formula is extensively used by experimentalists for the planning and interpretation of experiments. Analytic formulae of the next section are also transparent. Since acceleration effects are treated in them exactly, they are valid under the same condition (2.12) as the Tamm original formula (2.14), but include, in addition, the charge finite acceleration (or deceleration). Another reason is that experimentalists want to know what they, in fact, measure. For this they need rather transparent analytic formulae to distinguish contributions from the uniform and accelerated (decelerated) charge motions. The formulae presented in the next section satisfy these requirements and may be used for the rough estimation of the acceleration effects. After this stage, the explicit formulae presented in this section may be applied (as it was done in [9]) to take into account the effect of finite distances. Our experience [9] tells us that exact numerical calculations without preliminary analytical consideration is not very productive.
In what follows, we intend to investigate the deviation from the Tamm formula arising from the charge deceleration. Let us consider particular cases.

3 Particular cases

3.1 Decelerated and accelerated motion on a finite interval

Let a charge move in the interval (z_1, z_2) according to the law shown in Fig. 1a :

$$z = z_1 + v_1(t-t_1) + \frac{1}{2}a(t-t_1)^2. \tag{3.1}$$

The motion begins at the moment t_1 and terminates at the moment t_2. The charge velocity varies linearly with time from the value $v = v_1$ at $t = t_1$ down to value $v = v_2$ at $t = t_2$: $v = v_1 + a(t-t_1)$. It is convenient to express the acceleration a and the motion interval through z_1, z_2, v_1, v_2:

$$a = \frac{v_1^2 - v_2^2}{2(z_1 - z_2)}, \quad t_2 - t_1 = \frac{2(z_2 - z_1)}{v_2 + v_1}.$$

For the treated case, function $\tau(z)$ entering into (2.1) is given by

$$\tau(z) = t_1 - 2v_1\frac{z_2 - z_1}{v_2^2 - v_1^2}[1 - (1 + \frac{z - z_1}{z_2 - z_1}\frac{v_2^2 - v_1^2}{v_1^2})^{1/2}]. \tag{3.2}$$

When the condition (2.12) is fulfilled (i.e., ψ_1 is of the form (2.13)), the radiation intensity can be taken in a closed form. For this we should evaluate integrals

$$I_c(z_1, v_1; z_2, v_2) = \int_{z_1}^{z_2} \cos\psi_1 dz, \quad \text{and} \quad I_s(z_1, v_1; z_2, v_2) = \int_{z_1}^{z_2} \sin\psi_1 dz \tag{3.3}$$

entering into (2.10). In a manifest form, they are given in Appendix. Using them, we evaluate the intensity of radiation:

$$\sigma_r(\theta) = \frac{e^2k^2n\sin^2\theta}{4\pi^2c}[(\int_{z_1}^{z_2} dz' \cos\psi_1\cdot)^2 + (\int_{z_1}^{z_2} dz' \sin\psi_1)^2] =$$

$$= \frac{e^2\sin^2\theta}{2\pi^2cn\cos^2\theta}\{1 - \cos(u_2^2 - u_1^2) + \pi\alpha^2[(C_2 - C_1)^2 + (S_2 - S_1)^2]\pm$$

$$\pm\sqrt{2\pi}\alpha[(C_2 - C_1)(\sin u_2^2 - \sin u_1^2) - (S_2 - S_1)(\cos u_2^2 - \cos u_1^2)]\}, \tag{3.4}$$

where we put

$$C_1 = C(u_1), \quad C_2 = C(u_2), \quad S_1 = S(u_1), \quad S_2 = S(u_2), \quad \alpha = [\frac{k(z_2 - z_1)}{n|\cos\theta(\beta_2^2 - \beta_1^2)|}]^{1/2},$$

$$u_1 = \sqrt{\frac{k(z_2 - z_1)n|\cos\theta|}{|\beta_2^2 - \beta_1^2|}}(\beta_1 - \frac{1}{n\cos\theta}), \quad u_2 = \sqrt{\frac{k(z_2 - z_1)n|\cos\theta|}{|\beta_2^2 - \beta_1^2|}}(\beta_2 - \frac{1}{n\cos\theta});$$

C and S are Fresnel integrals defined as

$$S(x) = \sqrt{\frac{2}{\pi}}\int_0^x dt \sin t^2 \quad \text{and} \quad C(x) = \sqrt{\frac{2}{\pi}}\int_0^x dt \cos t^2.$$

Plus and minus signs in (3.4) refer to $\cos\theta > 0$ and $\cos\theta < 0$, respectively. Further, $\beta_1 = v_1/c$ and $\beta_2 = v_2/c$.

When $v_1 \to v_2 = v$, the intensity (3.4) goes into the Tamm formula (2.14) in which one should put $t_0 = (z_2 - z_1)/2v$.

Figure 2 demonstrates angular radial distributions for the fixed initial velocity $\beta_1 = 1$ and different final velocities β_2. The length of the sample was chosen $L = 0.5cm$, the wavelength $\lambda = 4\cdot10^{-5}cm$, the refractive index of the sample $n = 1.392$. For β_2 close to β_1 ($\beta_2 = 0.99$), the angular distribution strongly resembles the Tamm one. When β_2 diminishes ($\beta_2 = 0.9$ and $\beta_2 = 0.8$), a kind of a plato appears. Its edges are at the Cherenkov angles corresponding to β_1 and β_2 ($\cos\theta_1 = 1/\beta_1 n$, $\cos\theta_2 = 1/\beta_2 n$). On the Cherenkov threshold ($\beta_2 = 1/n$), σ_r has a peculiar form with fast oscillations at large angles. This form remains the same for the velocities below the Cherenkov threshold, but the oscillations are washed out for $\beta_2 = 0$.

On the other hand, we can put $\beta_2 = 0$ and change β_1. The case $\beta_1 = 1$ is shown in

Fig. 2d. The curves corresponding to other β_1 are shown in Fig. 3. The angular dependences of the radial intensity are always smooth for $\beta_2 = 0$. the main maximum of the radiation is at $\cos\theta = 1/\beta_1 n$ which coincides with the Cherenkov radiation condition. This means that under certain circumstances the bremsstrahlung can imitate the Cherenkov radiation. Formerly, this fact was admitted in [11] for small changes ($v_1 - v_2 << v_1$) of the charge velocity.
It was shown explicitly [12], in the time representation, that for the accelerated charge motion, the Cherenkov-like shock wave arises at the moment when the charge velocity coincides with the light velocity in medium. Then, the content of this section may be viewed as the translation of [12] into the frequency language (which is more frequently used by experimentalists).
The calculations of this section were performed with analytical formula (3.3) which is valid both for the decelerated ($v_1 > v_2$) and accelerated ($v_2 > v_1$) charge motion in medium. As far as we know, it is obtained here for the first time. The results of this section may be useful for the studying of the Cherenkov radiation arising from the decelerated heavy ions motion in medium (for them the energy losses are large due to large atomic number) [13].

3.2 Simplest superposition of accelerated, decelerated, and uniform motions

We also consider another problem corresponding to the motion shown in Fig. 1b. A charge is at rest at the space point $z = -z_0$ up to a moment $t = -t_0$. In the time interval $-t_0 < t < -t_1$, it moves with acceleration a up to reaching the velocity v at the space point $z = -z_1$:

$$z = -z_0 + \frac{1}{2}a(t + t_0)^2, \quad v(t) = a(t + t_0).$$

In the time interval $-t_1 < t < t_1$, a charge moves with the constant velocity v: $z = vt$. Finally, in the time interval $t_1 < t < t_0$, a charge moves with deceleration a up to reaching the state of rest at the moment t_0 at the space point $z = z_0$:

$$z = z_0 - \frac{1}{2}a(t - t_0)^2, \quad v(t) = -a(t - t_0).$$

It is convenient to express t_0, t_1, and a through z_0, z_2 and v:

$$a = \frac{v^2}{2(z_0 - z_1)}, \quad t_0 = \frac{2z_0 - z_1}{v}, \quad t_1 = \frac{z_1}{v}.$$

After the moment $t = t_0$, the charge is at rest at the point $z = z_0$.
Neglecting the terms of the order $1/k_n r$ and higher outside the ψ_1 function, one gets for the radial intensity

$$\sigma_r(\omega) = \frac{e^2 k^2 r^4 n \sin^2\theta}{4\pi^2 c}(I_c I_c' + I_s I_s'). \tag{3.5}$$

Here $I_c = \sum_i I_c^{(i)}$, $I_s = \sum_i I_s^{(i)}$, $(I_c)' = \sum_i (I_c^{(i)})'$, $(I_s)' = \sum_i (I_s^{(i)})'$, where

$$I_c^{(i)} = \int dz' \frac{1}{R^2} \cos\psi_i, \quad I_s^i = \int dz' \frac{1}{R^2} \sin\psi_i$$

$$(I_c^i)' = \int dz' \frac{r - z'\cos\theta}{R^3} \cos\psi_i, \quad (I_s^i)' = \int dz' \frac{r - z'\cos\theta}{R^3} \sin\psi_i, \quad i = 1,2,3,$$

where $\psi_i = kn(R - r) + \tau_i$ and $R = (r^2 + z'^2 - 2rz'\cos\theta)^{1/2}$. The superscripts $1,2$ and 3 refer to the the accelerated $(-z_0 < z' < -z_1)$, uniform $(-z_1 < z' < z_1)$, and decelerated $(z_1 < z' < z_0)$ parts of a charge trajectory. The functions $\tau_i(z)$ entering into ψ_i are equal to

$$\tau_1 = -\frac{2z_0 - z_1}{v} + \frac{2}{v}\sqrt{(z + z_0)(z_0 - z_1)} \quad \text{for} \quad -z_0 < z < -z_1,$$

$$\tau_2 = \frac{z}{v} \quad \text{for} \quad -z_1 < z < z_1,$$

$$\tau_3 = \frac{2z_0 - z_1}{v} - \frac{2}{v}\sqrt{(z_0 - z)(z_0 - z_1)} \quad \text{for} \quad z_1 < z < z_0. \tag{3.6}$$

If the motion interval $L = 2z_0$ is much smaller than the radius r of the observation sphere, then

$$I_c = I_c' = \sum_i I_c^{(i)} =, \quad I_s = I_s' = \sum_i I_s^{(i)},$$

$$I_c^{(i)} = \frac{1}{r^2}\int dz' \cos\psi_i, \quad I_s^{(i)} = \frac{1}{r^2}\int dz' \sin\psi_i, \quad i = 1,2,3$$

and

$$\sigma_r(\theta) = \frac{e^2k^2r^4n\sin^2\theta}{4\pi^2c}[(I_c)^2 + (I_s)^2], \tag{3.7}$$

If, in addition, the condition (2.12) is fulfilled, then

$$I_c = I_c(-z_0, 0; -z_1, v) + I_c(-z_1, v; z_1, v) + I_c(z_1, v; z_0, 0),$$

$$I_s = I_s(-z_0, 0; -z_1, v) + I_s(-z_1, v; z_1, v) + I_s(z_1, v; z_0, 0), \tag{3.8}$$

where the functions $I_c(z_1, v_1; z_2, v_2)$ and $I_s(z_1, v_1; z_2, v_2)$ are the same as in Eq.(3.3) (they were explicitly written out in Appendix). Due to the symmetry of the problem,

$$I_s(-z_0, 0; -z_1, v) = -I_s(z_1, v; z_0, 0), \quad I_c(-z_0, 0; -z_1, v) = I_(z_1, v; z_0, 0),$$

$$I_s(-z_1, v; z_1, v) = 0, \quad I_c(-z_1, v; z_1, v) = \frac{2\beta}{(1 - \beta n\cos\theta)} \sin[\frac{\omega z_1}{v}(1 - \beta n\cos\theta)], \tag{3.9}$$

Using (3.7), we evaluated a number of angular dependences for the $\beta = 1$ and various values of z_1 (Figs. 4 and 5). Each of these figures contains three curves

depicting the total intensity σ_t given by (3.7), its bremstrahlung part σ_{BS} obtained by dropping in (3.8) the term $I_c(-z_1, v; z_1, v)$ corresponding to the uniform motion on the interval $(-z_1, z_1)$, and the Tamm intensity σ_T obtained by dropping in (3.8) the terms $I_c(-z_0, 0; -z_1, v)$ and $I_c(z_1, v; z_0, 0)$ corresponding to the non-uniform motion. For the motion shown in Fig.1(b) u_1 and u_2 are given by

$$u_1 = -\sqrt{k(z_0 - z_1)n|\cos\theta|}\frac{1}{\beta n\cos\theta}, \quad u_2 = \sqrt{k(z_0 - z_1)n|\cos\theta|}(1 - \frac{1}{\beta n\cos\theta}).$$

It follows from this that for $z_1 \to z_0$ (this corresponds to the zero interval for the non-uniform motion), $u_1 \to 0$, $u_2 \to 0$ and (see Appendix) $I_c(-z_0, 0; -z_1, v)$ and $I_c(z_1, v; z_0, 0)$ also tend to zero (despite the fact that acceleration and deceleration become infinite in this limit), and the whole intensity is reduced to the contribution arising from a charge uniform motion on the interval $(-z_0, z_0)$. The parameter x_1 in Figs. 4 and 5 means z_1/z_0. It shows on which part of the total path a charge moves uniformly. For example, $x_1 = 0.999$ means uniform and non-uniform motions take place on 0.999 and 0.001 parts of the total motion path, respectively.

We turn to Fig.4a corresponding to $x_1 = z_1/z_0 = .999$. We see that the total intensity σ_t coincides with the Tamm one σ_T only in the immediate neighbourhood of the main maximum (which, in turn, consists of many peaks). To the right of this maximum, the intensity of the BS radiation practically coincides with the Tamm one, while the total intensity is much smaller. To the left of main maximum, σ_t practically coincides with σ_{BS}, while σ_T is by an order smaller. This looks more pronounced for $x_1 = 0.99$, where the total and bremsstrahlung intensities increase to the left of main maximum . Let $x_1 = 0.9$ (Fig. 4c). We observe that σ_{BS} coincides with σ_T to the right of the main maximum and with σ_t to the left of it. At the main maximum, σ_t, σ_{BS} and σ_T are of the same order. This picture remains the same for smaller x_1, up to $x_1 = 0.1$ (Fig. 4 d). Beginning from $x_1 = 0.01$, the Tamm intensity begins to decrease in maximum (Fig. 5 a). This is more pronounced for smaller x_1 (Fig.5b) where it is shown that for $x_1 = 0.001$, both σ_T and σ_{BS} begin to oscillate to the right of main maximum (Fig. 5b). For very small x_1, σ_T degenerates into

$$\sigma_T(\theta) = \frac{4e^2nz_1^2}{\lambda^2 c}\sin^2\theta$$

while σ_{BS} coincides with σ_t everywhere except for large angles, where σ_{BS} is very small (Fig. 5 c). Finally, for $x_1 = 0$, σ_T is zero and $\sigma_{BS} = \sigma_t$ (Fig. 5 d).

What can we learn from these figures?

1. The total intensity coincides with BS to the left of main maximum.
2. The Tamm formula satifactorily describes BS to the right of the main radiation maximum.
3. The Tamm formula coincides with the total intensity only in the immediate vicinity of the main maximum. It sharply disagrees with BS and with the total intensity to the left of the main maximum.
4. The bremsstrahlung maximum is approximately at the angle $\cos\theta = 1/\beta n$ coinciding with the Cherenkov radiation angle. This takes place even for Fig. 5 (d)

which describes the accelerated and decelerated charge motions and does not include the uniform motion.
5. The radiation from accelerated and decelerated paths of the charge trajectory tends to zero when the lengths of these paths tend to zero (despite the infinite acceleration and deceleration). There are no jumps of the charge velocity for arbitrary small (yet, finite) acceleration and deceleration paths. Therefore, in this limit, the Tamm formula describes the radiation of a charge uniformly moving on the finite interval without recourse to the acceleration and deceleration contributions at the ends of the motion interval. However, some reservation is needed. Although there are no jumps of velocity and the acceleration is everywhere finite, there are jumps of acceleration at the moments corresponding to the beginning and termination of motion and at the moments when the uniform and non-uniform charge motions meet with each other. At these moments, the third order time derivatives of the charge trajectory are infinite and they, in principle, can give contribution to the Tamm formula. To exclude this possibility, the everywhere continuous charge trajectory should be considered (this is in progress now).
The problem treated in this section describes the same physical situation as the original Tamm problem (see Introduction). Since in reality acceleration and deceleration exhibited by a charge are always finite, the problem treated in this section is more physical.
To the best our knowledge, the analytic formula (3.7) describing the charge uniform and accelerated motion and generalizing the Tamm formula, is obtained here for the first time.
It should be noted that, in the time representation, the space-time evolution of the shock waves arising in the treated problem was studied formerly in [9]. It was shown there that a complex consisting of the Cherenkov shock wave and the shock wave (not bremsstrahlung shock wave) closing the Cherenkov cone is created at the moment when the charge velocity coincides with the light velocity in medium. On the part of trajectory, corresponding to the uniform charge motion (Fig. 1(b)), this complex propagates with the light velocity in medium without changing its form. On the decelerated part of the charge trajectory it leaves the charge at the moment when the charge velocity again coincides with the light velocity in medium. After this moment, it propagates with the light velocity in medium. In this section, meeting the experimentalists demands, we translated results of [9] into the frequency language. In fact, experimentalists ask the questions like these: how much photons with the frequency ω should be observed, what is their angular distribution? Analytic formulae of this section answer these questions.

3.3 More complicated superposition of accelerated, decelerated, and uniform motions

We also consider another problem corresponding to the motion shown in Fig. 1 c. This is needed to investigate how the radiation intensity changes when the velocity

v_2 changes from the value above c_n to the value below it. A charge is at rest at the space point $z = -z_0$ up to a moment $t = -t_0$. In the time interval $-t_0 < t < -t_1$, it moves with acceleration a up to reaching the velocity v_1 at the space point $z = -z_1$:

$$z = -z_0 + \frac{1}{2}a(t + t_0)^2, \quad v = a(t + t_0).$$

It is convenient to express t_1 and a through z_1 and v_1:

$$a = \frac{v_1^2}{2(z_0 - z_1)}, \quad t_0 - t_1 = \frac{2(z_0 - z_1)}{v_1}.$$

In the time interval $-t_1 < t < -t_2$, a charge moves with deceleration a up to reaching the velocity v_2 at the space point $z = -z_2$:

$$z = -z_1 + v_1(t + t_1) - \frac{1}{2}a(t + t_1)^2, \quad v = a(t + t_1).$$

It is convenient to express t_2 and z_2 through v_2:

$$z_2 = z_0 - (z_0 - z_1)(2 - \frac{\beta_2^2}{\beta_1^2}), \quad t_2 = t_0 - 2\frac{2v_1 - v_2}{v_1^2}(z_0 - z_1). \tag{3.10}$$

In the time interval $-t_2 < t < t_2$ a charge moves uniformly with the velocity v_2 up to reaching the space point $z = z_2$:

$$z = -z_2 + v_2(t + t_2), \quad v = v_2.$$

Therefore, $z_2 = v_2 t_2$. Substituting z_2 and t_2 from (3.10), we find t_0

$$t_0 = \frac{1}{v_2}[z_0 - (z_0 - z_1)(2 - 4\frac{v_2}{v_1} + \frac{v_2^2}{v_1^2})].$$

In the time interval $t_2 < t < t_1$, a charge moves with acceleration a up to reaching the velocity v_1 at the space point $z = z_1$:

$$z = z_2 + v_2(t - t_2) + \frac{1}{2}a(t - t_2)^2, \quad v = v_2 + a(t - t_2).$$

Finally, in the time interval $t_1 < t < t_0$, a charge moves with deceleration a up to reaching the state of rest at the moment t_0 at the space point $z = z_0$:

$$z = z_1 + v_1(t - t_1) - \frac{1}{2}a(t - t_1)^2, \quad v = v_1 - a(t - t_1).$$

After the moment t_0, the charge is at rest at the point $z = z_0$. For that motion, the Fourier transform of the current density reduces to the following sum

$$j_\omega = \frac{e}{2\pi}\delta(x)\delta(y)[\Theta(z+z_0)\Theta(-z-z_1)\exp(-i\omega\tau_1) + \Theta(z+z_1)\Theta(-z-z_2)\exp(-i\omega\tau_2) +$$

$$\Theta(z+z_2)\Theta(z_2-z)\exp(-i\omega\tau_3)+\Theta(z-z_2)\Theta(z_1-z)\exp(-i\omega\tau_4)+$$
$$+\Theta(z-z_1)\Theta(z_0-z)\exp(-i\omega\tau_5)],$$

where

$$\tau_1=-t_0+\frac{2}{v_1}\sqrt{(z+z_0)(z_0-z_1)},\quad \tau_2=-t_0+\frac{2}{v_1}[2(z_0-z_1)-\sqrt{(z_0-z_1)(z_0-z-2z_1)}],$$

$$\tau_3=\frac{z}{v_2},\quad \tau_4=t_0-\frac{2}{v_1}[2(z_0-z_1)-\sqrt{(z_0-z_1)(z_0+z-2z_1)}],$$

$$\tau_5=t_0-\frac{2}{v_1}\sqrt{(z_0-z)(z_0-z_1)}. \tag{3.11}$$

If the conditions $knr >> 1$, $L << r$ and (2.12) are fulfilled, then radiation intensity can be evaluated analytically:

$$\sigma_r(\omega)=\frac{e^2\sin^2\theta}{n\pi^2c}[(I_c)^2+(I_s)^2], \tag{3.12}$$

where:

$$I_c=I_c(-z_0,0;-z_1,v_1)+I_c(-z_1,v_1;-z_2,v_2)+I_c(-z_2,v_2;z_2,v_2)+$$
$$I_c(z_2,v_2;z_1,v_1)+I_c(z_1,v_1;z_0,0),$$
$$I_s=I_s(-z_0,0;-z_1,v_1)+I_s(-z_1,v_1;-z_2,v_2)+I_s(-z_2,v_2;z_2,v_2)+$$
$$I_s(z_2,v_2;z_1,v_1)+I_s(z_1,v_1;z_0,0).$$

Again, due to the symmetry of the problem

$$I_c(-z_0,0;-z_1,v_1)=I_c(z_1,v_1;z_0,0),\quad I_c(-z_1,v_1;-z_2,v_2)=I_c(z_2,v_2;z_1,v_1),$$

$$I_c(-z_2,v_2;z_2,v_2)=\frac{2\beta_2}{(1-\beta_2 n\cos\theta)}\sin[\frac{\omega z_2}{v_2}(1-\beta_2 n\cos\theta)],$$

$$I_s(-z_0,0;-z_1,v_1)=-I_s(z_1,v_1;z_0,0),\quad I_s(-z_1,v_1;-z_2,v_2)=-I_s(z_2,v_2;z_1,v_1),$$
$$I_s(-z_2,v_2;z_2,v_2)=0,\quad I_s=0.$$

Now we choose $\beta_1=1$, $z_1=0.99$ and change β_2. The case $\beta_2=1$ is shown in Fig. 4b. Smaller values of β_2 are shown in Fig. 6. Consider Fig. 6 a, corresponding to $\beta_2=0.8$. We see that the Cherenkov maximum $\theta_{Ch}=\arccos(1/\beta_2 n)$ is shifted relative to the BS maximum. Like in Figs. 4 and 5, we observe that the Tamm formula satisfactorily describes bremsstrahlung in the backward part of the angular spectrum (for $\beta=0.8$ this agreement begins from $\theta\approx 50^0$). The total intensity is satisfactorily reproduced by the BS intensity everywhere in the forward angular region ($0<\theta<50^0$) except for the immediate neighbourhood of the Cherenkov angle. In this angular region, the Tamm formula disagrees both with total and BS intensities everywhere except for angles close to the Cherenkov one. An important case is $\beta_2=$

$1/n$ corresponding to the Cherenkov threshold (Fig. 6 b). The total intensity has two maxima of the same magnitude: one corresponding to the Cherenkov maximum (at $\theta = 0^0$) and other corresponding to the bremsstrahlung maximum. For β_2 below the Cherenkov threshold, the Cherenkov maximum disappears (Fig. 6 c), while the Tamm intensity decreases coinciding at large angles with that of BS. In the forward direction, the total intensity does not differ from the BS one. Finally, for $\beta_2 = 0$, the Tamm intensity disappears, while the total intensity coincides with the BS one (Fig. 6 d).

What can we learn from this section? There are two characteristic velocities β_1 and β_2 in Fig. 6. Correspondingly, there are two Cherenkov maxima defined by $\cos\theta = 1/\beta_1 n$ and $\cos\theta = 1/\beta_1 n$ when both β_1 and β_1 are greater than $1/n$ (Fig. 6 (a,b)). When β_2 becomes smaller than $1/n$, only one Cherenkov maximum corresponding to $\cos\theta = 1/\beta_1 n$ survives (Fig. 6 (c,d)).

The formula (3.12) describing the radiation intensity on the charge trajectory shown in Fig. 1 (c) is obtained here for the first time.

4 Analytic estimates

In this section, the radiation intensities written out in a previous section in terms of Fresnel integrals, will be expressed through elementary functions. This is possible when the arguments of Fresnel integrals are large. Physically, this means that the product kl_a is large (k is the wave number and l_a is is the space interval where a charge moves non-uniformly).

For the motion shown in Fig. 1(a) and corresponding to $\beta_1 n > 1$ and $\beta_2 n > 1$, one finds that for $k(z_2 - z_1) >> 1$ the radiation intensity is given by:

$$\sigma_r = \frac{e^2 n \sin^2\theta}{\pi^2 c}\{\frac{1}{4}[\frac{\beta_2 - \beta_1}{(1-\beta_1 n\cos\theta)(1-\beta_2 n\cos\theta)}]^2 + \\ + \frac{\beta_1\beta_2}{(1-\beta_1 n\cos\theta)(1-\beta_2 n\cos\theta)}\sin^2\frac{\psi}{2}\} \qquad (4.1)$$

for $0 < \theta < \theta_2$ and $\theta > \theta_1$. Here we put

$$\cos\theta_1 = 1/\beta_1 n, \quad \cos\theta_2 = 1/\beta_2 n, \quad \psi = 2\frac{k(z_2 - z_1)}{\beta_1 + \beta_2}(\frac{\beta_1 + \beta_2}{2} n\cos\theta - 1).$$

On the other hand, for $\theta_2 < \theta < \theta_1$ one has

$$\sigma_r = \sigma_r(4.1) + \frac{e^2\sin^2\theta}{\pi c n\cos^2\theta}\{\alpha^2 + \frac{\alpha n\cos\theta}{\sqrt{2\pi}}[\beta_2\frac{\cos u_2^2 - \sin u_2^2}{\beta_2 n\cos\theta - 1} - \beta_1\frac{\cos u_1^2 - \sin u_1^2}{\beta_1 n\cos\theta - 1}]\}, \quad (4.2)$$

where α, u_1 and u_2 are the same as in (3.4). The term proportional to α^2 is much larger than other ones everywhere except for the angles close to θ_1 and θ_2. For these angles the above expansion of Fresnel integrals fails (since u_1 and u_2 vanish at these

angles). These formulae mean that radiation intensity oscillates with decreasing amplitude for $0 < \theta < \theta_2$ and $\theta > \theta_1$ and decreases rather slowly like

$$\frac{e^2\alpha^2 \sin^2\theta}{\pi c n \cos^2\theta} \tag{4.3}$$

for $\theta_2 < \theta < \theta_1$. The oscillating terms (first term in (4.2) and the term proportional to α) are much smaller than (4.3). Exactly such behaviour of σ_r with maxima at θ_1 and θ_2 and a rather flat region between them demonstrates Fig. 2(b).

For $\beta_2 = 1/n$, above formulae predict intensity oscillations for $\theta > \theta_1$ and their absence for $\theta < \theta_1$ (see Fig. 2 (c)).

A particular interesting case having numerous practical applications corresponds to the complete termination of motion ($\beta_2 = 0$) . In this case,

$$\sigma_r = \frac{e^2 n \beta_1^2}{4\pi^2 c} \frac{\sin^2\theta}{(1-\beta_1 n \cos\theta)^2} \tag{4.4}$$

for $\theta > \theta_1$ and

$$\sigma_r = \sigma_r(4.4) + \frac{e^2 \sin^2\theta}{\pi c n \cos^2\theta}[\alpha^2 - \frac{\beta_1 \alpha n \cos\theta}{\sqrt{2\pi}} \frac{\cos u_1^2 - \sin u_1^2}{\beta_1 n \cos\theta - 1}] \tag{4.5}$$

for $\theta < \theta_1$. Here α and u_1 are the same as in (3.4) if one puts $\beta_2 = 0$ in them:

$$\alpha = \frac{1}{\beta_1}\sqrt{\frac{k(z_2 - z_1)}{n\cos\theta}}, \quad u_1 = \sqrt{k(z_2 - z_1) n \cos\theta}(1 - \frac{1}{\beta_1 n \cos\theta}).$$

There are no intensity oscillations for $\theta > \theta_1$ and very small oscillations for $\theta < \theta_1$ (they are due to the last term in (4.5)). Figures 2(d) and 3 agree with this prediction.

We clarify now why the radiation intensities disappear for $\theta > \theta_c$ for the motion shown in Fig. 1 (b). For this aim we should evaluate the integrals $I_c = \int v d\tau \cos\psi$ and $I_s = \int v d\tau \sin\psi$ entering into (3.6). In terms of Fresnel integrals, they are given in Appendix. Due to to the symmetry of the treated problem, I_s=0 while I_c is reduced to

$$I_c = I_c^a + I_c^d + I_c^u = 2I_c^a + I_c^u. \tag{4.6}$$

Here I_c^a, I_c^d and I_c^u are the integrals over the accelerated ($-z_0 < z < -z_1$), decelerated ($z_1 < z < z_0$) and uniform ($-z_1 < z < z_1$) parts of a charge trajectory, respectively. Again, it was taken into account that $I_c^a = I_c^d$ due to the symmetry of the problem. The integral I_c^u corresponding to the uniform motion on the interval ($-z_1 < z < z_1$) is

$$I_c^u = \frac{2\beta}{k(1-\beta n\cos\theta)} \sin[\frac{k z_1}{\beta}(1 - \beta n \cos\theta)]. \tag{4.7}$$

Then, for $\theta < \pi/2$, one gets (see Appendix)

$$I_c^a = \int_{-z_0}^{-z_1} dz \cos\psi = \frac{1}{kn\cos\theta}\{\sin(u_2^2 - \gamma) - \sin(u_1^2 - \gamma) +$$

$$+\alpha\sqrt{2\pi}[\cos\gamma(C_2 - C_1) + \sin\gamma(S_2 - S_1)]\}. \tag{4.8}$$

For the motion shown in Fig.1 (b), u_1, u_2, α and γ are given by

$$u_1 = -\sqrt{k(z_0 - z_1)n\cos\theta}\frac{1}{\beta n\cos\theta}, \quad u_2 = \sqrt{k(z_0 - z_1)n\cos\theta}(1 - \frac{1}{\beta n\cos\theta}),$$

$$\alpha = \frac{1}{\beta}[\frac{k(z_0 - z_1)}{n\cos\theta}]^{1/2}, \quad \gamma = kz_0 n\cos\theta + \frac{k(z_0 - z_1)}{\beta^2 n\cos\theta} - \frac{k(2z_0 - z_1)}{\beta}.$$

Changing Fresnel integrals by their asymptotic values, we get for $k(z_0 - z_1) >> 1$ and $\theta < \theta_c$ ($\cos\theta_c = 1/\beta n$):

$$I_c^a = -\alpha\sqrt{2\pi}\frac{\cos\gamma + \sin\gamma}{kn\cos\theta} + \frac{\beta n}{k(\beta n\cos\theta - 1)}\sin[kz_1(1 - \beta n\cos\theta)]. \tag{4.9}$$

To obtain I_c, one should double I_c^a (since $I_c^a = I_c^d$) and add I_c^u given by (4.7). This gives

$$I_c = 2I_c^a + I_c^u = -\alpha\sqrt{2\pi}\frac{\cos\gamma + \sin\gamma}{kn\cos\theta} \quad \text{and}$$

$$\sigma_r = \frac{e^2}{2\pi cn^2\beta^2}k(z_0 - z_1)\frac{\sin^2\theta}{\cos^3\theta}(1 + \sin 2\gamma). \tag{4.10}$$

We see that for $\theta < \theta_c$ the part of I_c^a is compensated by the Tamm amplitude I_c^u. In this angular region the oscillations are due to the $(1 + \sin 2\gamma)$ factor. For $\theta > \theta_c$, one finds

$$I_c^a = \frac{\beta n}{k(\beta n\cos\theta - 1)}\sin[kz_1(1 - \beta n\cos\theta)]. \tag{4.11}$$

Inserting (4.7) and (4.11) into (4.6), we find

$$I_c = 2I_c^a + I_c^u = 0 \quad \text{and} \quad \sigma_r = 0.$$

We see that for $\theta > \theta_c$ the summary contribution of the accelerated and decelerated parts of the charge trajectory is compensated by the contribution of its uniform part. The next terms arising from the expansion of Fresnel integrals are of the order $1/k(z_0 - z_1)$ and, therefore, are negligible for $k(z_0 - z_1) >> 1$. This behaviour of radiation intensities is confirmed by Fig. 4.

The disappearance of the radiation intensity for $\theta > \theta_c$ takes place for arbitrary z_1 satisfying conditon $z_0 - z_1 >> 0$ and, particularly, for $z_1 = 0$. In this case, there is no uniform motion and accelerated motion at the interval $-z_0 < z < 0$ is followed by the decelerated motion on the interval $0 < z < z_0$. Equations (4.10) and (4.11) with $z_1 = 0$ in them qualitatively describe Fig. 5 corresponding to the small length of uniform motion. It should be stressed again that these estimates are not valid near the angles θ_1 and θ_2 where the arguments of the Fresnel integrals vanish.

5 Back to the original Tamm problem

5.1 Exact solution

Let a charge be at rest at the point $z = -z_0$ up to a moment $t = -t_0$. In the time interval $-t_0 < t < t_0$, it moves with the constant velocity v. Finally, after the moment t_0, it is again at rest at the point $z = z_0$. The corresponding charge and current densities are

$$\rho(t) = e\delta(x)\delta(y)[\delta(z+z_0)\Theta(-t-t_0)+\delta(z-z_0)\Theta(t-t_0)+\delta(z-vt)\Theta(t+t_0)\Theta(t_0-t)],$$

$$\vec{j} = j\vec{n}_z, \quad j = v\delta(z-vt)\Theta(t+t_0)\Theta(t_0-t), \quad t_0 = \frac{z_0}{v}.$$

Their Fourier transforms are

$$\rho(\omega) = \frac{1}{2\pi}\int \rho(t)\exp(-i\omega t)dt = \rho_1(\omega)+\rho_2(\omega)+\rho_3(\omega), \quad j(\omega) = v\rho_3(\omega), \qquad (5.1)$$

where

$$\rho_1(\omega) = -\frac{e}{2\pi i\omega}\delta(z+z_0)\delta(x)\delta(y)[\exp(i\omega t_0)-\exp(i\omega T)],$$

$$\rho_2(\omega) = -\frac{e}{2\pi i\omega}\delta(z-z_0)\delta(x)\delta(y)[\exp(-i\omega T)-\exp(-i\omega t_0)],$$

$$\rho_3(\omega) = \frac{e}{2\pi v}\delta(x)\delta(y)\Theta(z+z_0)\Theta(z_0-z)\exp(-i\omega z/v), \quad j = v\rho_3.$$

In (5.1), the integration over t is performed from $-T$ to T, where $T > t_0$. Later, we take the limit $T \to \infty$. Electromagnetic potentials are equal to

$$\Phi(\omega) = \Phi_1(\omega)+\Phi_2(\omega)+\Phi_3(\omega), \quad A(\omega) \equiv A_z(\omega) = \epsilon\mu\beta\Phi_3(\omega), \qquad (5.2)$$

where

$$\Phi_1(\omega) = -\frac{e}{2\pi i\omega\epsilon}[\exp(i\omega t_0)-\exp(i\omega T)]\frac{\exp(-ik_nR_1)}{R_1},$$

$$\Phi_2(\omega) = -\frac{e}{2\pi i\omega\epsilon}[\exp(-i\omega T)-\exp(-i\omega t_0)]\frac{\exp(-ik_nR_2)}{R_2},$$

$$\Phi_3(\omega) = \frac{e}{2\pi v\epsilon}\int_{-z_0}^{z_0}\frac{dz'}{R}\exp(-\frac{i\omega z'}{v})\exp(-ik_nR).$$

Here $R_1 = [(z+z_0)^2+\rho^2]^{1/2}$, $R_2 = [(z-z_0)^2+\rho^2]^{1/2}$, $R = [(z-z')^2+\rho^2]^{1/2}$, $k_n = \omega/c_n$, $c_n = c/n$ is the light velocity in medium, n is its refractive index.
These potentials satisfy the gauge condition

$$div\vec{A}+\frac{\epsilon\mu}{c}\frac{\partial\Phi}{\partial t} = 0, \quad \text{while} \quad div\vec{A}+\frac{\epsilon\mu}{c}\frac{\partial\Phi_3}{\partial t} \neq 0.$$

Thus, Φ_1 and Φ_2 should be taken into account. Another argument for this is to evaluate

$$E_r = -\frac{\partial \Phi}{\partial r} - \frac{i\omega}{c} A_r, \quad A_r = A\cos\theta.$$

It is easy to check that E_r decreases like $1/r^2$ for $r \to \infty$, while it decreases like $1/r$ if Φ is substituted by Φ_3. Thus, Φ_1 and Φ_2 are needed to guarantee the correct asymptotic behaviour of electromagnetic field strengths (if we evaluate $\vec{E}$ according to $\vec{E} = -\nabla\Phi - i\omega\vec{A}/c$).

We are primarily interested in the radial energy flux $S_r \sim E_\theta H_\phi$. In the expression

$$E_\theta = -\frac{1}{r}\frac{\partial \Phi}{\partial \theta} - \frac{i\omega}{c} A_\theta, \quad A_\theta = -\sin\theta A,$$

the first term is the $1/kr$ part of the second term and, therefore, it can be disregarded (since in realistic conditions kr is about 10^7). Thus obtained E_θ differs from the exact E_θ by terms of the order $1/kr$.

To make clear the physical meaning of electromagnetic potentials (5.2), we rewrite them in the time representation:

$$\Phi(t) = \int \exp(i\omega t)\Phi(\omega)d\omega, \quad \Phi(t) = \Phi_1(t) + \Phi_2(t) + \Phi_3(t), \quad A(t) = \epsilon\mu\beta\Phi_3(t),$$

$$\Phi_1(t) = \frac{e}{\epsilon R_1}\Theta[R_1 - c_n(t+t_0)], \quad \Phi_2(t) = \frac{e}{\epsilon R_2}\Theta[c_n(t-t_0) - R_2],$$

$$\Phi_3(t) = \frac{e}{\epsilon v}\int_{-z_0}^{z_0} \frac{dz'}{R}\delta(t - \frac{z'}{v} - k_n R), \quad R = [(z-z')^2 + \rho^2]^{1/2}. \tag{5.3}$$

When evaluating $\Phi_1(t)$ and $\Phi_2(t)$, it was taken into account that

$$\int_{-\infty}^{\infty} \exp(i\omega x)d\omega/\omega = i\pi sign(x).$$

The following notation will be useful: the spheres $R_1 \equiv [\rho^2 + (z+z_0)^2]^{1/2}$ and $R_2 \equiv [\rho^2 + (z-z_0)^2]^{1/2}$ will be denoted by S_1 and S_2. We say that a particular space point lies inside or outside S_1 if $R_1 < c_n(t+t_0)$ and $R_1 > c_n(t+t_0)$, respectively. And, similarly, for S_2.

We see that $\Phi_1(t)$ differs from zero outside the sphere S_1, i.e., at those points which are not reached by the information about the beginning of motion. Further, $\Phi_2(t)$ differs from zero inside the sphere S_2, i.e., at those points which are reached by the information about the termination of motion. Or, in other words, Φ_1 and Φ_2 describe electrostatic fields of a charge which rests at the point $z = -z_0$ up to a moment $t = -t_0$ (beginning of motion) and at the point $z = z_0$ after the moment $t = t_0$ (termination of motion). In what follows, electrostatic fields associated with Φ_1 and Φ_2 will be denoted by E_1 and E_2, respectively.

To evaluate $\Phi_3(t)$, we use the well-known relation

$$\delta[f(z)] = \sum_i \frac{\delta(z - z_i)}{|f'(z_i)|},$$

where the summation runs over all roots of the equation $f(z) = 0$ and

$$f'(z_i) = \frac{df(z')}{dz'}|_{z=z_i}.$$

The roots of the equation

$$t - \frac{z'}{v} = \frac{R}{c_n}, \quad R = [(z - z')^2 + \rho^2]^{1/2}. \tag{5.4}$$

Squaring this equation, we obtain quadratic equation relative z' with the roots

$$z_1 = \gamma_n^2(vt - z\beta_n^2 - \beta_n R_m), \quad z_2 = \gamma_n^2(vt - z\beta_n^2 + \beta_n R_m), \quad \gamma_n^2 = \frac{1}{1 - \beta_n^2}. \tag{5.5}$$

Here $R_m = [(z - vt)^2 + (1 - \beta_n^2)\rho^2]^{1/2}$.

5.1.1 Charge velocity is smaller than the light velocity in medium

Consider first the case when $\beta_n < 1$. Then, only z_1 root satisfies (5.4) (the appearance of the second root is due to the fact that the quadratic equation following from (5.4) can have roots which do not satisfy (5.4)). Now we impose the condition $-z_0 < z_1' < z_0$ which means that the motion takes place on the interval $(-z_0, z_0)$. Then, it follows from (5.4), that $\Phi_3(t) \neq 0$ for the space points lying inside S_1 and outside S_2:

$$\Phi_3(t) = \frac{e}{R_m \epsilon}\Theta[c_n(t + t_0) - R_1]\Theta[R_2 - c_n(t - t_0)], \quad t_0 = \frac{z_0}{v}. \tag{5.6}$$

Physically, Φ_3 describes the EMF of a charge moving on the interval $(-z_0, z_0)$. It differs from zero at those space points which obtained information on the beginning of motion and did not obtain information on its termination. It is easy to see that for $\beta_n < 1$, the S_2 sphere lies entirely inside S_1, i.e., there are no intersections between them. The positions of S_1 and S_2 spheres for two different moments of time are shown in Fig. 7. The region where $\Phi_3 \neq 0$ is between S_1 and S_2 belonging to the same t. Static fields Φ_1 and Φ_2 lie outside S_1 and inside S_2, respectively.

5.1.2 Charge velocity is greater than the light velocity in medium

Let now $\beta_n > 1$. Then, Φ_1, Φ_2 and their physical meanings are the same as for $\beta_n < 1$. We turn now to Φ_3. It is easy to check that two roots satisfy (4.4) if $z < vt$, and there are no roots if $z > vt$. We need further notation. We denote by L_1 and L_2

the straight lines $z = -z_0 + \rho|\gamma_n|$ and $z = z_0 + \rho|\gamma_n|$, respectively (Fig. 8). We say that a particular point is to the left or right of L_1 if $z < -z_0+\rho|\gamma_n|$ or $z > -z_0+\rho|\gamma_n|$, respectively. And similarly, for L_2. Correspondingly, a particular point lies between L_1 and L_2 if $-z_0+\rho|\gamma_n| < z < z_0+\rho|\gamma_n|$. L_1 and L_2 are inclined toward the motion axis under the Cherenkov angle $\theta_{Ch} = \arccos(1/\beta_n)$. The Cherenkov shock wave (CSW) is the straight line $z+\rho/|\gamma_n| = vt$, perpendicular both to L_1 and L_2 straight lines and enclosed between them. We observe that denominators R_m vanish exactly for $z + \rho/|\gamma_n| = vt$, i.e., on the CSW. There are no other zeroes of R_m. We say also that a particular point lies under or above the Cherenkov shock wave (CSW) if $z + \rho/|\gamma_n| < vt$ or $z + \rho/|\gamma_n| > vt$, respectively.
We impose the condition for motion to be on the interval $(-z_0, z_0)$. Then, the first root exists in the following space-time domains (Fig. 7, d):
i) To the right of L_2, it exists only outside S_1 and inside S_2;
ii) Between L_1 and L_2, it exists outside S_1 and under the CSW.
The contribution of the first root to Φ_3 is:

$$\Phi_3^{(1)} = \frac{e}{\epsilon R_m}\{\Theta(z + z_0 - \rho|\gamma_n|)\Theta(z_0 + \rho|\gamma_n| - z)\Theta(t - \frac{z+\rho/|\gamma_n|}{v})+$$

$$+\Theta(z - z_0 - \rho|\gamma_n|)\Theta[c_n(t - t_0) - R_2)]\}\Theta[R_1 - c_n(t + t_0)]. \qquad (5.7)$$

The first term in (5.7) is singular on the CSW (since $R_m = 0$ on it) enclosed between L_1 and L_2 straight lines. The second term in (5.7) does not contain singularities.
Now we turn to the second root:
i) To the left of the L_1, it exists only inside S_1 and outside S_2.
ii) Between L_1 and L_2, it exists outside S_2 and under the CSW.
Correspondingly, the contribution of the second root is

$$\Phi_3^{(2)} = \frac{e}{\epsilon R_m}\{\Theta(z + z_0 - \rho|\gamma_n|)\Theta(z_0 + \rho|\gamma_n| - z)\Theta(t - \frac{z+\rho/|\gamma_n|}{v})+$$

$$+\Theta(\rho|\gamma_n| - z - z_0)\Theta[c_n(t + t_0) - R_1)]\}\Theta[R_2 - c_n(t - t_0)]. \qquad (5.8)$$

Only the first term in this expression is singular on the same CSW.

The contribution of two roots to Φ_3 is

$$\Phi_3 = \Phi_3^{(1)} + \Phi_3^{(2)}. \qquad (5.9)$$

In Fig. 8 (a,b,c) there are shown positions of S_1, S_2 and CSW shock waves at different moments of time. In Fig. 7 (d), which is a magnified image of Fig. 7(b), we see five regions where EMF differs from zero. The region 1 lies outside S_1 and S_2 and above CSW. There is only the electrostatic field E_1 there. In the region 2 lying inside S_1 and S_2, there is only the electrostatic field E_2. In the region 3 lying inside S_1 and outside S_2, there is EMF of a moving charge (only the 2-nd root contributes). In the region 4 lying inside S_2 and outside S_1, there is EMF of a moving charge (only the 1-nd root contributes) and electrostatic fields E_1 and E_2. Finally, in the region

5 lying outside S_1 and S_2 and under CSW, there is EMF of a moving charge (both roots contribute) and electrostatic field E_1.

So far we suggested that for $t < -t_0$ and $t > t_0$, a charge is at rest at points $z = -z_0$ and $z - z_0$, respectively. However, usually, when dealing with the Tamm problem, one uses only the vector potential desribing the charge motion on the interval $(-z_0 < z < z_0)$. It is given by $A = \mu\epsilon\beta\Phi_3$. Then, one evaluates the magnetic and electric fields using the relations: $\mu\vec{H} = curl\vec{A}$ and $curl\vec{H} = i\epsilon k\omega\vec{E}$ valid in the ω representation. In this case, terms Φ_1 and Φ_2 drop out from consideration. Then, there are nonzero electromagnetic potentials corresponding to the first root in region 4, the second root in region 3 and first and second roots in region 5. In other space regions, potentials are zero. On the border of regions 3, 4 and 5 with regions 1 and 2, potentials exhibit jumps, and, therefore, field strengths have delta- type singularities.

In the previous section, the uniform charge motion on a finite interval (corresponding to the Tamm problem) is followed or preceeded by the accelerated motion (see Fig. 1 (b)). Since there are no jumps of velocities on the borders of the above regions, the δ-type singularities of EMF strengths arising from the beginning (termination) of the uniform motion are partly compensated by the singularities of EMF strengths corresponding to the non-uniform motion termination (beginning) at the point where uniform and non-uniform motions meet. When the deceleration region diminishes, the contribution from decelerated parts of a trajectrory diminishes also (Fig. 4) and the Tamm intensity becomes closer to the total one.

We conclude: the vector potential $A = \beta\mu\epsilon\Phi_3$ corresponds to the charge motion on a finite $(-z_0, z_0)$ interval and does not contain the instantaneous acceleration effects. They are equal to zero according to the results of section 3.
Experimentalists insist that they measure $\vec{E}(\omega)$ and $\vec{H}(\omega)$ (in fact, they detect photons with a definite frequency). It is just the reason that enabled us to operate in sections 2-3 with the Fourier transforms $\vec{E}(\omega)$ and $\vec{H}(\omega)$.

5.2 The Tamm approximate solution

The Tamm vector potential in the Fourier representation is

$$A_T(\omega) = \frac{e}{\pi r n\omega(\cos\theta - 1/\beta_n)} \exp(-ik_n r)\sin[k_n z_0(\cos\theta - 1/\beta_n)]. \qquad (5.10)$$

It is obtained from (2.2) when (i)-(iii) conditions of section 2 are fulfilled. Using (5.10) for the evaluation of field strentghs and the radiation intensity, one gets the famous Tamm formula (2.5). Going in (5.10) to the time representation, one gets

$$A_T(t) = \frac{e}{rn|\cos\theta - 1/\beta_n|}\times$$

$$\times[\Theta(\frac{1}{\beta_n} - \cos\theta)\cdot\Theta(r - r_1)\cdot\Theta(r_2 - r) + \Theta(\cos\theta - \frac{1}{\beta_n})\cdot\Theta(r - r_2)\cdot\Theta(r_1 - r)]. \quad (5.11)$$

Here

$$r_1 = c_n t + z_0(\frac{1}{\beta_n} - \cos\theta), \quad \text{and} \quad r_2 = c_n t - z_0(\frac{1}{\beta_n} - \cos\theta).$$

For $\beta_n < 1$, (5.11) is transformed into

$$A_T(t) = \frac{e}{rn(1/\beta_n - \cos\theta)} \cdot \Theta(r - r_2)\Theta(r_1 - r), \tag{5.12}$$

that is, the electromagnetic field differs from zero between two non-intersecting curves S_1 and S_2 defined by $r = r_1$ and $r = r_2$, respectively. (Fig. 9 (a)).

On the other hand, for $\beta_n > 1$,

$$A_T(t) = \frac{e}{rn(\cos\theta - 1/\beta_n)}\Theta(r - r_1) \cdot \Theta(r_2 - r) \tag{5.13}$$

for $\cos\theta > 1/\beta_n$ and

$$A_T(t) = \frac{e}{rn(1/\beta_n - \cos\theta)}\Theta(r - r_2) \cdot \Theta(r_1 - r) \tag{5.14}$$

for $\cos\theta < 1/\beta_n$. For $\beta_n > 1$, the curves S_1 and S_2 are intersected at $\cos\theta = 1/\beta_n$. The region where $A_T(t) \neq 0$ lies between S_1 and S_2 (Fig.9 (b)). By comparing this figure with Fig. 8, we observe that the Cherenkov shock wave shown in Fig. 8 by the thick line and enclosed between L_1 and L_2 straight lines is degenerated into a point coinciding with the intersection of curves 1 and 2. These intersection points at different moments of time lie on the same straight line L inclined towards the motion axis under the Cherenkov angle $\cos\theta_{Ch} = 1/\beta n$. The electromagnetic potentials and field strengths are infinite on this line at the distance $r = c_n t$ from the origin and, therefore, the major part of the energy flux propagates under the angle θ_{Ch} towards the motion axis (Fig. 9 (b))

For $\beta_n > 1$, the curves S_1 and S_2 are always intersected at large distances (where the Tamm approximation holds). Probably, this fact and the absence of the Cherenkov cone (similar to that of the previous section) gave rise to a number of attempts [4,5] to interpret the Tamm intensity (2.5) as the interference between BS shock waves emitted at the boundary $z = \pm z_0$ points. The standard approach [2] associates (5.11) with the radiation produced by a charge uniformly moving in medium with the velocity $v > c_n$. We believe that this dilemma cannot be resolved in the framework of the Tamm approximate solution (5.10).

The question arises: at which stage the Cherenkov shock wave has dropped from the vector potential (5.10)? We have shown above that it is present both in (5.3) and (5.9). But (5.3) is just the Fourier transform of $A(\omega)$ defined in (5.2). The Tamm vector potential (5.10) is obtained from the exact (5.2) by changing $R \to r$ in the denominator and $R \to r - z' \cos\theta$ in the exponent. The first approximation is not essential if the observation distance is much larger than the motion interval. It is the second approximation that is responsible for the disappearance of the Cherenkov shock wave. Condition for the validity of the (iii) approximation of section 2 is

not fulfilled in realistic cases. Exact analytical and numerical calculations show that an enormous broadening of the angular intensity spectrum takes place in the spectral representation [8, 12]. In the time representation, this broadening leads to the appearance of the Cherenkov shock wave enclosed between L_1 and L_2 straight lines shown in Fig. 8. Formerly, equations similar to (5.6)-(5.9) were obtained in [6] but without using spectral representation (5.2) as an intermediate step. The latter is needed to recover at what stage of approximations, the Cherenkov shock wave drops out from consideration and to make a choice between opposite interpretations of the Tamm formula for radiation intensity.

6 Discussion

In Fig. 10, there are shown positions of shock waves at the moment $t = 0$ lying inside the interval $-t_0 < t < t_0$. At this moment, S_1 shock wave associated with the beginning of motion has arisen, but S_2 shock wave associated with the termination of motion has not still appeared. In this figure, we see the part of a Cherenkov wave, enclosed between the motion axis and S_1, tangential to the latter and having a normal inclined under the angle $\theta_{Ch} = \arccos(1/\beta n)$ toward the motion axis. Since S_2 shock wave is absent, the appearance of CSW cannot be attributed to the interference of S_1 and S_2 waves. Therefore, in the time representation, the existence of the S_2 shock wave is not needed for the appearance of the Cherenkov shock wave. In some time interval the Cherenkov shock wave is enclosed between the motion axis and the shock wave S_1. (Figs. 8 (a) and 10). As time goes, the S_2 shock wave arises. After this moment, the Cherenkov shock wave is tangential to S_1 and S_2 and is enclosed between them (Fig. 8, (b)-(d)).

Since the frequency distribution of the radiation intensity $\sigma_r(\omega)$ involves integration over all times, all particular configurations shown in Fig. 8 contribute to $\sigma_r(\omega)$. Thus, it is still possible to associate the Tamm formula (2.5) with the interference of S_1 and S_2 shock waves (one may argue that, since all times contribute to the radiation intensity in the spectral representation, the large times, when S_1 and S_2 shock waves are intersected, also give contribution to the just mentioned frequency representation). However, as it was shown analytically and numerically in the framework of the spectral representation (see section (3.2)), the contribution of accelerated and decelerated paths of the charge trajectory tend to zero when the lengths of these paths tend to zero. In this limit, the total radiation intensity coincides with the Tamm one (2.5). Therefore, the Tamm formula for the intensity of radiation cannot be reduced to the interference of BS shock waves (since their contribution tends to zero in this limit). We see that only the combined treatment of the Tamm problem in the time and frequency representations permitted us to discriminate between two above mentioned interpretations of the Tamm formula.

However, the following topics concerning the Tamm problem still remain unclear for us. We illustrate them using Figs. 2-5 corresponding to the typical experimental situations.

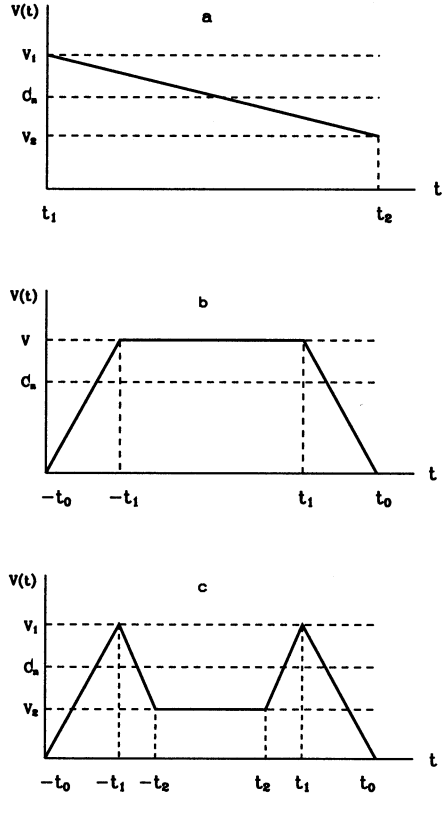

Fig. 1. Time dependences of charge velocities treated in the text.
a: Charge deceleration on a finite interval; v_1, v_2 and c_n are the charge initial and final velocities and light velocity in medium, respectively.
b: Charge acceleration followed by the uniform motion and deceleration. This case allows one to estimate contributions to the radiation intensity from the accelerated, uniform, and decelerated parts of a charge trajectory.
c: This motion permits one to estimate how the radiation intensity changes when the transition from the velocity greater to the velocity smaller than the light velocity in medium takes place.

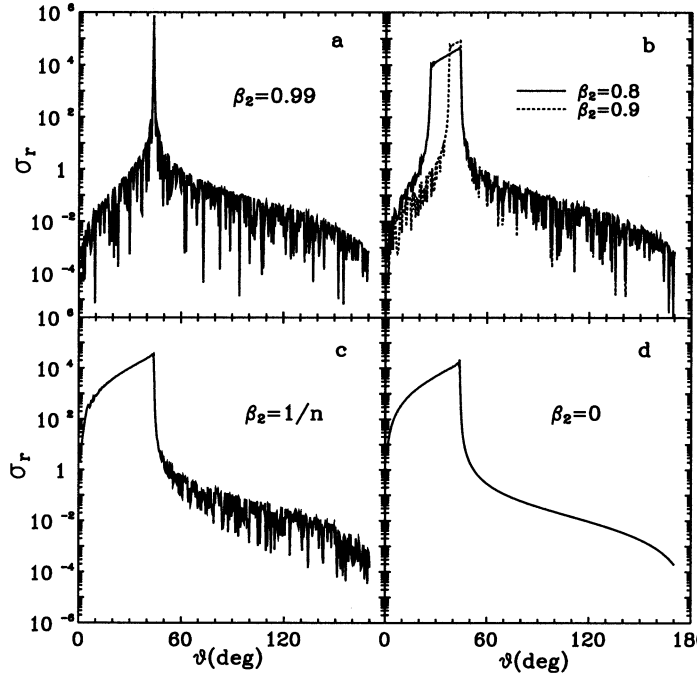

Fig. 2. Radiation intensities (in units e^2/c) corresponding to Fig. 1 (a) for $\beta_1 = 1$ fixed and various β_2. For $\beta_2 = 0.99$ (a), the radiation spectrum is close to that described by the Tamm formula (3.4). For smaller β_2 (b), a kind of plato appears in the radiation intensity. Its edges are at the Cherenkov angles corresponding to β_1 and β_2. For $\beta_2 = 1/n$, the distribution of radiation has a specific form (c) without oscillations to the left of the maximum. This form remains essentially the same for smaller β_2, but the tail oscillations are washed out (d). In all these cases, the main radiation maximum is at $\cos\theta = 1/\beta_1 n$. All these results are confirmed analytically in section 4. These intensities were evaluted for the following parameters: the wavelength $\lambda = 4 \cdot 10^{-5} cm$, the motion length $L = 0.5 cm$, the refractive index $n = 1.392$.

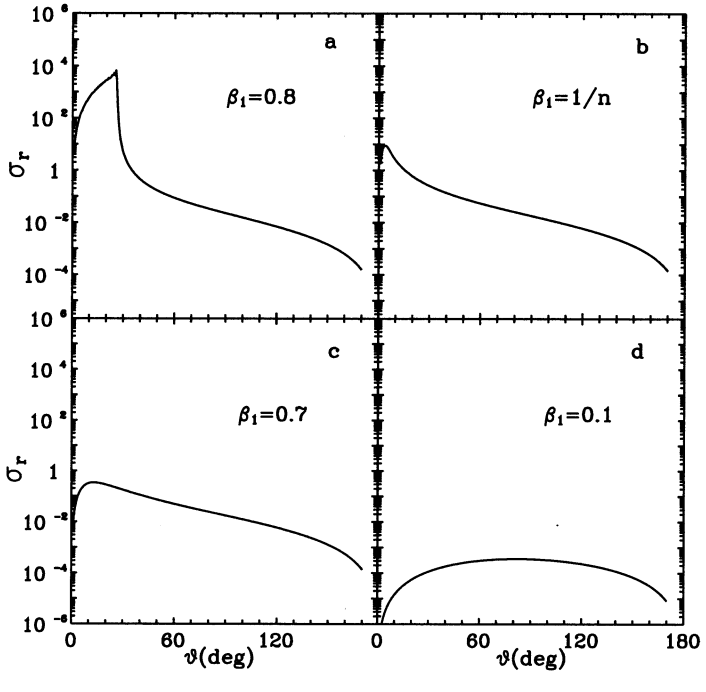

Fig. 3. Radiation intensities corresponding to Fig. 1 (a) for $\beta_2 = 0$ fixed and various β_1. For $\beta_1 = 1$, the radiation spectrum is shown in Fig. 2(d). For smaller β_1, the intensity maximum shifts to smaller angles (a) reaching zero angle at the Cherenkov threshold $\beta_1 = 1/n$ (b). The maximum is at the Cherenkov angle corresponding to β_1. Below the Cherenkov threshold, the form of radiation spectrum remains practically the same, but its amplitude decreases (c,d). Other parameters are the same as in Fig. 2.

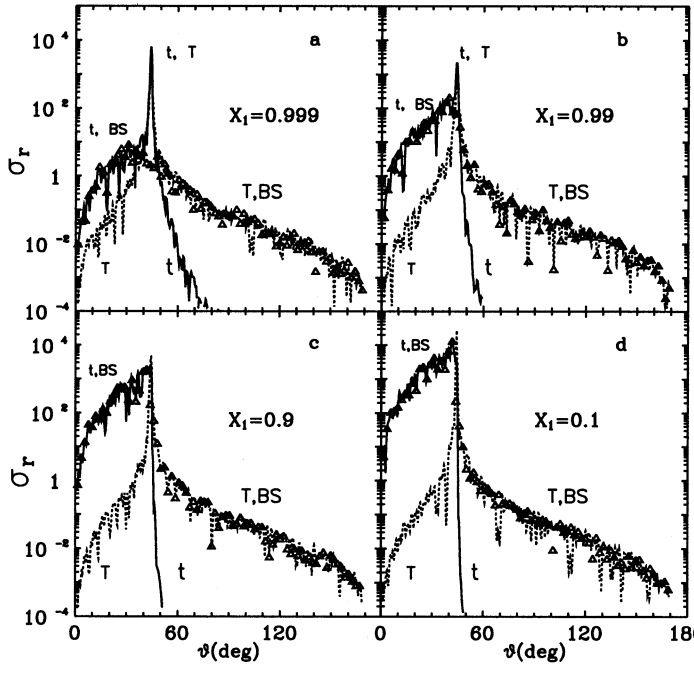

Fig. 4. Radiation intensities corresponding to Fig. 1 (b) for $\beta = 1$ and various z_1. Here $x_1 = z_1/z_0$ is the part of a charge trajectory on which it moves uniformly. Other parameters are the same as in Fig. 2. Solid and dotted lines refer to the total intensity and the intensity associated with the charge uniform motion on the interval $(-z_1, z_1)$, respectively. Triangles refer to the intensity associated with a charge non-uniform motion on the intervals $(-z_0, -z_1)$ and (z_1, z_0). Since these lines are overlapped, we supplied them with letters t (total), T (Tamm) and BS (bremsstrahlung). To make radiation intensities more visible, we averaged them over three neighbouring points, thus, considerably smoothing the oscillations. The same is true for Figs. 5 and 6. The main maximum of the total radiation intensity is at the Cherenkov angle defined by $\cos\theta = 1/\beta n$. Its sudden drop above this angle is due to the interference of Cherenkov and bremsstrahlung radiations (see section 4).

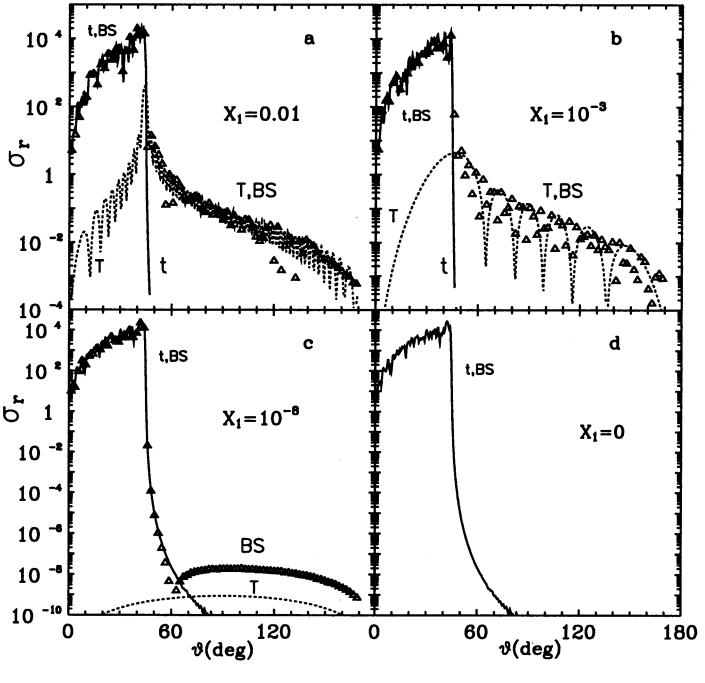

Fig. 5. The same as in Fig. 4, but for smaller x_1. It is seen that with the diminishing of the uniform motion interval, the Tamm radiation intensity tends to zero, while the total intensity approaches the bremsstrahlung one. Again, the main maximum of the total radiation intensity is at the Cherenkov angle defined by $\cos\theta = 1/\beta n$.

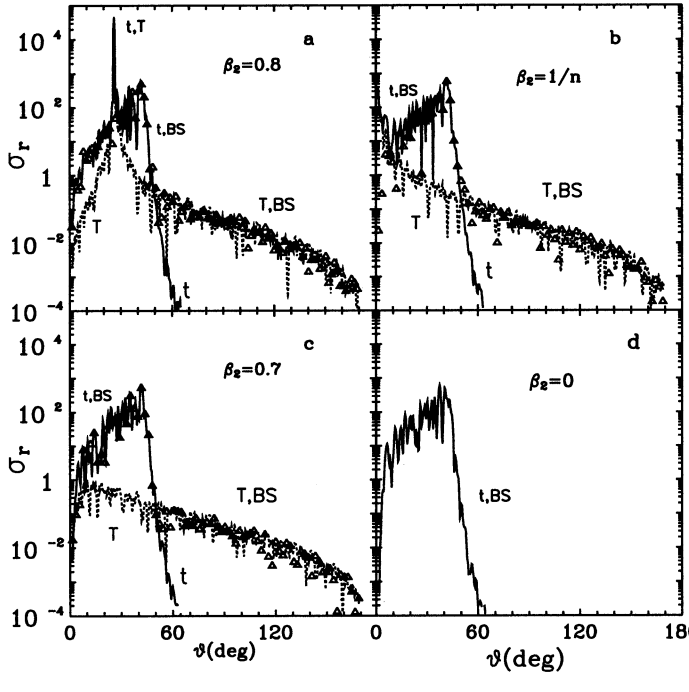

Fig. 6. Total, Tamm and bremsstrahlung radiation intensities corresponding to Fig. 1 (c) for $\beta = 1, x_1 = 0.99$ and various β_2. The case $\beta_2 = 1$ is considered in Fig. 4 (b). Other parameters are the same as in Fig. 2. For β_1 and β_2 greater than $1/n$ the total intensity has two maxima at the Cherenkov angles defined by $\cos\theta = 1/\beta_1 n$ and $\cos\theta = 1/\beta_2 n$ (a, b). At the Cherenkov threshold, these maxima have the same height. For $\beta_2 < 1/n$, only one maximum corresponding to $\cos\theta = 1/\beta_1 n$ survives (c,d). For $\beta_2 = 0$, the Tamm intensity is zero, and $\sigma_t = \sigma_{BS}$.

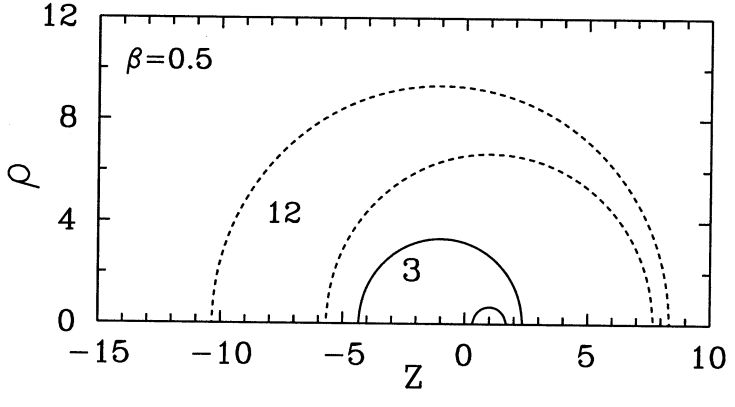

Fig. 7. Positions of Bremsstrahlung shock waves for $T = 3$ and $T = 12$ in the exact Tamm problem for the case when the charge velocity ($\beta = 0.5$) is smaller than the light velocity in medium. Here $T = ct/z_0$. The vector potential differs from zero between solid lines for $T = 3$ and between dotted lines for $T = 12$; ρ and z are in units z_0. The motion interval and refractive index are: $L = 0.5cm$ and $n = 1.5$, respectively.

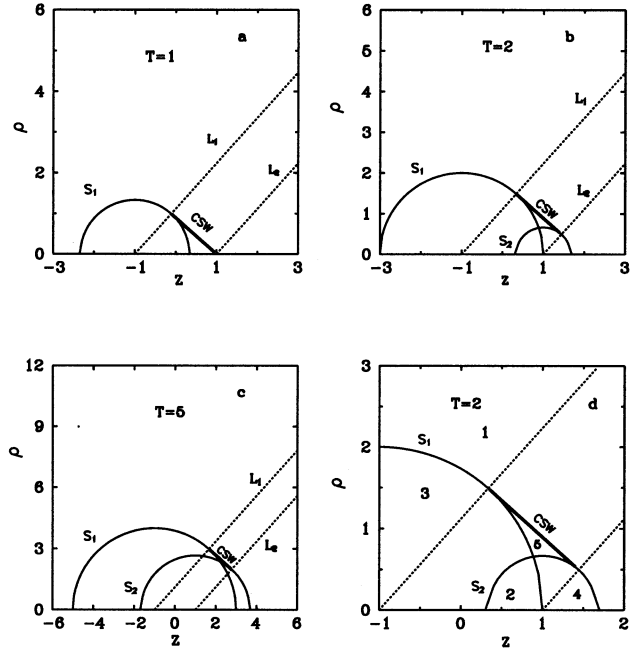

Fig. 8. Time evolution of shock waves in the exact Tamm problem for the case when the charge velocity ($\beta = 1$) is greater than the light velocity in medium. S_1 and S_2 are shock waves radiated at the beginning and termination of motion, respectively. CSW is the Cherenkov shock wave. The time $T = 1$ corresponds to the moment when S_2 wave arises(a) . For larger times, CSW is tangential both to S_1 and S_2 and is confined between straight lines L_1 and L_2 (b,c). Part (d) of the figure is a magnified version of (b). The vector is zero in region 2 lying inside S_1 and S_2 and in region 2 lying outside S_1 and S_2 and above CSW. Only one retarded time contributes in region 3 (lying inside S_1 and outside S_2) and in region 4 (lying inside S_2 and outside S_1). Two retarded times contribute to region 5 lying ouside S_1 and S_2 and below CSW. Other parameters are the same as in Fig. 7.

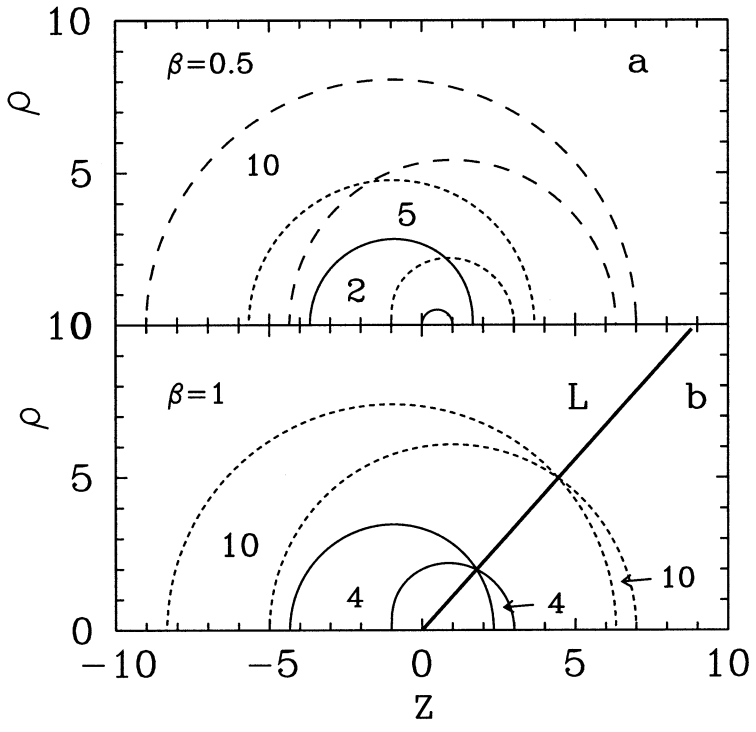

Fig. 9 (a): Time evolution of shock waves corresponding to the Tamm approximate vector potential (5.12) for the case when the charge velocity is smaller than the light velocity in medium. The Tamm potential differs from zero between two solid lines for $T = 2$, between two dotted lines for $T = 5$ and between two dashed lines for $T = 10$.
(b): The same as in (a), but for the charge velocity greater than the light velocity in medium. The Tamm potential (5.13) and (5.14) differing from zero between two solid lines for $T = 4$ and between two dotted lines for $T = 10$, is singular at the intersection of lines with the same T. The straight line passing through these singular points is shown by a thick line. The energy flux propagates mainly along this straight line. Probably, the absence of CSW in this approximate picture has given rise to associate above singularities with an interference of BS shock waves. Other parameters are the same as in Fig. 7.

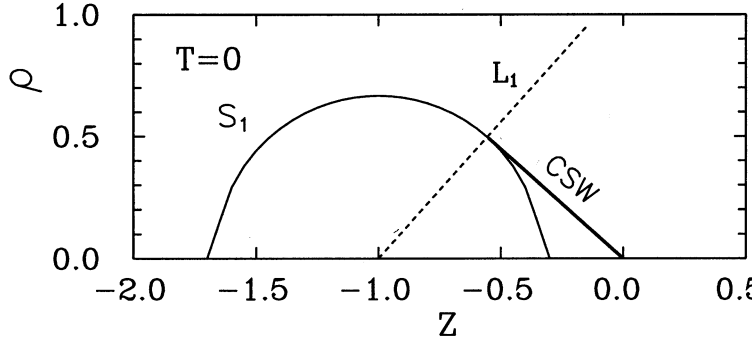

Fig. 10: A counter-example showing that in the exact Tamm model, the presence of two bremsstrahlung waves is not needed for the existence of the Cherenkov shock wave. In the time interval $-t_0 < t < t_0$, there is a shock wave S_1 arising at the beginning of motion and the Cherenkov shock wave CSW. The S_2 shock wave is not still appeared. Other parameters are the same as in Fig. 7.

1. Figure 4, corresponding to the charge trajectory shown in Fig. 1(b), demonstrates that to the right of the Cherenkov maximum, the Tamm and bremsstrahlung intensities almost coincide, while the total intensity is very small there. This means that the Tamm and bremsstrahlung amplitudes enter into (3.7) with opposite signs and almost compensate each other. Analytic consideration of section 4 aupports this claim. What is the physical reason for this?
2. Figure 3 and 5, corresponding to charge trajectories shown in Fig. 1 (a) and (b), repectively, show that the maximum of the bremsstrahlung intensity is always at the angle $\cos\theta = 1/\beta n$ coinciding with Cherenkov condition for the radiation. This takes place even in the absence of uniform motion (Figs. 2, 3, 5(d) and 6(d)). Again, analytic consideration of section 4 supports this. A possible answer gives consideration [12] of the accelerated charge motion in the time representation where the Cherenkov-like shock wave arises when the charge velocity coincides with the light velocity in medium.
3. The appearance of two Cherenkov maxima (Fig. 2 (b)), corresponding to the initial and final charge velocity and supported analytically in section 4, is rather unexpected.

7 Conclusion

We briefly summarize main results obtained:
1. The analytical solution describing accelerated (decelerated) charge motion in medium (Fig. 1 (a)) is found. The total radiation intensity has one maximum at the Cherenkov angle corresponding to β_1 (see Fig. 2(a,c,d)) or two maxima at the Cherenkov angles corresponding to β_1 and β_2 (Fig. 2(b)). This solution may be applied to study the radiation produced by electrons moving uniformly in heavy-water reactors (the electron arising from the β decay of some nucleus, moves with deceleration and, then is absorbed by another nucleus). Another possible application are experiments with heavy ions moving in medium [13] (due to large atomic numbers, the energy losses for heavy ions are also large).
2. We have found analytical expressions for the electromagnetic field and the energy flux radiated by a charge moving along the trajectory which consists of accelerated, decelerated, and uniform motion parts (Fig. 1 (b)). It is shown that when the lengths of accelerated and decelerated parts tend to zero, their contribution to the radiated energy flux also tends to zero despite the infinite value of acceleration along them. This means, in particular, that the original Tamm problem describing charge motion on a finite interval does not in fact contain the instantaneous acceleration and deceleration, as it is usually believed The total radiation intensity has a maximum at the Cherenkov angle defined by $\cos\theta = 1/\beta n$ (Figs. 4 and 5). The possible applications of this model are the same as those of the original Tamm problem (see Introduction).
3. Analytical expressions are obtained for the electromagnetic field and the energy flux radiated by a charge moving along the trajectory shown in Fig. 1(c). The

total radiation intensity has two maximuma at the Cherenkov angles defined by $\cos\theta = 1/\beta_1 n$ and $\cos\theta = 1/\beta_2 n$ if both β_1 and β_2 are greater than $1/n$ (Fig. 6 (a,b)). Only one maximum corresponding to $\cos\theta = 1/\beta_1 n$ survives if $\beta_2 < 1/n$ (Fig. 6 (c,d)).

4. We have also considered an alternative interpretation [4,5] of the Tamm radiation intensity formula (2.14) as an interference of two instantaneous bremsstrahlungs arising at the beginning and end of motion. It is shown that in the framework of the approximate solution found by Tamm, it is very hard to discriminate between its standard interpretation and one suggested in [4,5]. On the other hand, this discrimination is possible if we treat the Tamm problem simultaneously in the time and frequency representations. This combined consideration shows that it is impossible associate the Tamm formula (2.5) with the interference of the above-mentioned instantaneous bremsstrahlungs. This should not be mixed with the Vavilov assertion [3] on the nature of radiation observed by Cherenkov. It follows from Figs. 3 and 4 that angular distributions corresponding to finite accelerations are highly non-symmetrical relative to the Cherenkov angle, while distributions described by the Tamm formula are almost symmetrical. The angular distributions observed by Cherenkov were also highly non-symmetrical (see, e.g., [14]). They strongly resemble radiation intensities shown in Fig. 2 (d) and Fig. 3 (a) and corresponding to the zero final energy.

8 Appendix

In this Appendix I_c and I_s everywhere mean

$$I_c(z_1, v_1; z_2, v_2) = \int_{z_1}^{z_2} \cos\psi_1 dz \quad \text{and} \quad I_s(z_1, v_1; z_2, v_2) = \int_{z_1}^{z_2} \sin\psi_1 dz,$$

respectively.. Here

$$\psi_1 = \omega\tau(z) - knz\cos\theta,$$

while $\tau(z)$ is given by (3.2). The motion begins at the point z_1, at the moment t_1 with the velocity v_1 and ends at the point $z_2 > z_1$ with the velocity v_2. There are four possibilities depending on the signs of $\cos\theta$ and $(v_1 - v_2)$. Obviously, $v_2 > v_1$ and $v_1 > v_2$ correspond to accelerated and decelerated motions, respectively; $\cos\theta > 0$ and $\cos\theta < 0$ correspond to the observation angles lying in front and back semispheres, respectively.

1) $v_2 > v_1, \quad \cos\theta > 0$

$$I_c = \frac{1}{kn\cos\theta}\{\sin(u_2^2 - \gamma) - \sin(u_1^2 - \gamma) + \alpha\sqrt{2\pi}[\cos\gamma(C_2 - C_1) + \sin\gamma(S_2 - S_1)]\},$$

$$I_s = \frac{1}{kn\cos\theta}\{\cos(u_2^2 - \gamma) - \cos(u_1^2 - \gamma) - \alpha\sqrt{2\pi}[\cos\gamma(S_2 - S_1) - \sin\gamma(C_2 - C_1)]\},$$

2) $v_2 > v_1, \quad \cos\theta < 0$

$$I_c = -\frac{1}{kn\cos\theta}\{\sin(u_2^2+\gamma) - \sin(u_1^2+\gamma) - \alpha\sqrt{2\pi}[\cos\gamma(C_2-C_1) - \sin\gamma(S_2-S_1)]\},$$

$$I_s = \frac{1}{kn\cos\theta}\{\cos(u_2^2+\gamma) - \cos(u_1^2+\gamma) + \alpha\sqrt{2\pi}[\cos\gamma(S_2-S_1) + \sin\gamma(C_2-C_1)]\},$$

3) $v_1 > v_2, \quad \cos\theta > 0$

$$I_c = -\frac{1}{kn\cos\theta}\{\sin(u_2^2+\gamma) - \sin(u_1^2+\gamma) + \alpha\sqrt{2\pi}[\cos\gamma(C_2-C_1) - \sin\gamma(S_2-S_1)]\},$$

$$I_s = \frac{1}{kn\cos\theta}\{\cos(u_2^2+\gamma) - \cos(u_1^2+\gamma) - \alpha\sqrt{2\pi}[\cos\gamma(S_2-S_1) + \sin\gamma(C_2-C_1)]\},$$

4) $v_1 > v_2, \quad \cos\theta < 0$

$$I_c = \frac{1}{kn\cos\theta}\{\sin(u_2^2-\gamma) - \sin(u_1^2-\gamma) - \alpha\sqrt{2\pi}[\cos\gamma(C_2-C_1) + \sin\gamma(S_2-S_1)]\},$$

$$I_s = \frac{1}{kn\cos\theta}\{\cos(u_2^2-\gamma) - \cos(u_1^2-\gamma) + \alpha\sqrt{2\pi}[\cos\gamma(S_2-S_1) - \sin\gamma(C_2-C_1)]\}.$$

Here $u_1, u_2, C_1 = C(u_1), C_2 = C(u_2), S_1 = S(u_1), S_2 = S(u_2)$ and α are the same as in Eq.(3.4) and

$$\gamma = \omega t_1 + \frac{k(z_2-z_1)}{(\beta_2^2-\beta_1^2)n\cos\theta} - kn\cos\theta\frac{\beta_2^2 z_1 - \beta_1^2 z_2}{\beta_2^2-\beta_1^2} - 2\beta_1\frac{k(z_2-z_1)}{(\beta_2^2-\beta_1^2)}.$$

Obviously, I_c and I_s are the elements from which the total radiation intensity for the charge motion consisting of any superposition of accelerated, decelerated and uniform parts can be constructed.

References

[1] Frank I.M., 1988, Vavilov-Cherenkov Radiation (Moscow, Nauka), In Russian.

[2] Tamm I.E., 1939, J.Phys. USSR, 1, 439.

[3] Vavilov S.I., 1934, Dokl. Akad, Nauk, 2, 8, 457.

[4] Zrelov V.P., Ruzicka J., 1989, Chech.J.Phys. B, 39, 368.

[5] Zrelov V.P., Ruzicka J., 1992, Chech.J.Phys., 42, 45.

[6] Afanasiev G.N., Beshtoev Kh. and Stepanovsky Yu.P., 1996, Helv. Phys. Acta, 69, 111-129; Afanasiev G.N., Kartavenko V.G. and Stepanovsky Yu.P., 1999, J.Phys. D, 32, 2029.

[7] Kuzmin E.S. and Tarasov A.V., 1993, JINR Rapid Communications, 4[61]-93, 64, Dubna, 1993.

[8] Afanasiev G.N., Shilov V.M., 2000, J. Phys.D, 33, 2931.

[9] Afanasiev G.N., Shilov V.M., 2000, Physica Scripta, 62, 326;

[10] Afanasiev G.N., Kartavenko V.G. and Ruzicka J., 2000, J.Phys. A, 33, 7585.

[11] Krupa L., Ruzicka J. and Zrelov V.P., Preprint JINR P2-95-281, Dubna, 1995.

[12] Afanasiev G.N., Eliseev S.M. and Stepanovsky Yu.P., 1998, Proc. Roy. Soc. Lond. A, 454, 1049; Afanasiev G.N. and Kartavenko V.G., 1999, Can. J. Phys., 77, 561.

[13] Ruzicka J. et. al., 2000, Nucl. Instr. Methods, A, 431, 148.

[14] Cherenkov P.A., 1944, Trudy FIAN, 2, 3-62.

Received on March 1, 2002.

Афанасьев Г. Н., Шилов В. М. Е2-2002-36
Черенковское излучение и излучение ускорения в задаче Тамма

Рассматривается движение заряда в среде на конечном интервале. Анализируются альтернативные попытки интерпретировать излучение, описываемое формулой Тамма, как интерференцию волн тормозного излучения, возникающих в начале и в конце движения. Точное решение задачи Тамма во временном представлении показывает, что в определенном интервале времени существуют только черенковская волна и волна тормозного излучения, связанная с началом движения, и отсутствует волна тормозного излучения, связанная с его окончанием. Это показывает, что во временном представлении черенковское излучение не обязательно связано с интерференцией волн тормозного излучения. В спектральном представлении рассматривается движение заряда, состоящее из ускоренного, равномерного и замедленного. Получены аналитические формулы для интенсивности излучения, соответствующие этому движению. При стремлении длины интервала, на котором происходит ускорение, к нулю, вклад ускорения в интенсивность излучения также стремится к нулю, несмотря на бесконечную величину ускорения. Это показывает, что исходная задача Тамма не содержит вклада ускорения (что обычно предполагается). Совместное решение задачи Тамма во временном и спектральном представлениях показывает, что упомянутая альтернативная интерпретация несостоятельна.

Работа выполнена в Лаборатории теоретической физики им. Н. Н. Боголюбова ОИЯИ.

Препринт Объединенного института ядерных исследований. Дубна, 2002

Afanasiev G. N., Shilov V. M. E2-2002-36
Cherenkov Radiation Versus Bremsstrahlung in the Tamm Problem

The charge motion in medium on a finite space interval is considered. We analyze recent alternative attempts to interpret the radiation described by the Tamm formula as an interference of two instantaneous accelerations arising at the beginning and termination of motion. Exact solution of the Tamm problem in the time representation shows that in some time interval, only the bremsstrahlung shock wave associated with the beginning of motion and the Cherenkov shock wave exist, and there is no bremsstrahlung shock wave associated with the end of motion. This proves that in the time representation the Cherenkov radiation is not necessarily related to the interference of initial and final bremsstrahlung shock waves. In the spectral representation, we consider the motion consisting of accelerated, decelerated, and uniform parts. Analytic formulae are obtained describing electromagnetic fields and radiation intensities corresponding to this motion. Approximating the instantaneous acceleration in the original Tamm problem by the acceleration on a finite path and then tending its length to zero, we prove that the radiation intensity produced on the accelerated part of the charge trajectory also tends to zero (despite the infinite value of acceleration in this limit). This means that in the original Tamm problem the instantaneous acceleration and deceleration do not contribute to the radiation intensity (as it is usually believed). It seems that only the combined consideration of the Tamm problem in the time and spectral representations shows that the above-mentioned alternative interpretation of the Cherenkov relation fails.

The investigation has been performed at the Bogoliubov Laboratory of Theoretical Physics, JINR.

Preprint of the Joint Institute for Nuclear Research. Dubna, 2002

Макет *Т. Е. Попеко*

ЛР № 020579 от 23.06.97.
Подписано в печать 08.04.2002.
Формат 60 × 90/16. Бумага офсетная. Печать офсетная.
Усл. печ. л. 2,5. Уч.-изд. л. 3,98. Тираж 425 экз. Заказ № 53214.

Издательский отдел Объединенного института ядерных исследований
141980, г. Дубна, Московская обл., ул. Жолио-Кюри, 6.